CUTOFF INSENSITIVE GUIDANCE

by

THOMAS WELLS DE SWARTE

B.S. Marquette University
(1961)

SUBMITTED IN PARTIAL FULFILLMENT
OF THE REQUIREMENT FOR THE
DEGREE OF MASTER OF SCIENCE

at the

MASSACHUSETTS INSTITUTE OF
TECHNOLOGY

September, 1971

Signature of Author _____

Department of Aeronautics
and Astronautics

Certified by

Thesis Advisor

Accepted by _____

Chairman, Departmental
Committee on Graduate Students

CUTOFF INSENSITIVE GUIDANCE

by

Thomas Wells DeSwarte

Submitted to the Department of Aeronautics and Astronautics on September, 1971 in partial fulfillment of the requirements for the degree of Master of Science

ABSTRACT

A space vehicle with no thrust termination control, must expend a fixed amount of energy and still meet specified trajectory requirements. Velocity uncertainties introduced by ending powered flight via fuel depletion require that the terminal thrust direction lie along a range insensitive direction. This thesis proposes several guidance schemes for solving the problem described above. Particular emphasis of the analysis is placed on a parabolic guidance law. The law is evaluated for terminal fuel depletion conditions for various conditions of excess fuel and trajectories. In addition, a straight line-circular arc scheme is proposed and an optimal law which minimizes the mean squared value of the anvular velocity is discussed.

Thesis Supervisor: James E. Potter

Title: Associate Professor of Aeronautics and Astronautics

ACKNOWLEDGMENTS

The author wishes to express his appreciation to his thesis advisor Professor James E. Potter and his thesis supervisor Mr. Peter B. Howard for their substantial and valuable technical advice. Their patience and encouragement during the pursuit of this study is gratefully acknowledged.

In addition, special appreciation goes to Linda Syatt for her skillful typing of the manuscript.

TABLE OF CONTENTS

TABLE OF CONTENTS (cont.)

LIST OF ILLUSTRATIONS

CHAPTER I

INTRODUCTION

1.1 Cut-Off Insensitive Guidance

The subject of this thesis is the development and analysis of control laws for a high performance rocket vehicle in vacuum flight for which there is no control of the thrust termination. Deletion of thrust termination mechanisms may be desirable in applications where weight, electrical complexity, and system interfaces are to be minimized.

Because no thrust termination control is assumed, the rocket engine must consume a given amount of fuel to end powered flight. The amount of velocity change (delta velocity or ΔV) imparted to the vehicle is a function of its thrust force and mass characteristics. The desired trajectory objectives of attaining the proper velocity in order to free-fall to an inertial point in a fixed time must then be met at or near the time of fuel depletion. Rocket engine anomalies and mass and fuel uncertainties limit the knowledge of the actual delta velocity introducing a substantial velocity error in the trajectory. This obstacle may be overcome by commanding the thrust axis of the vehicle to be in an insensitive direction at the time of thrust termination. The insensitive direction

is defined as the direction along which incremental velocity errors may be introduced while still meeting the desired trajectory objectives.

The velocity which is required in order that the vehicle free-fall to a pre-selected point in a fixed time is defined as the correlated velocity ($\underline{V}_c$). The additional velocity required is

$$\underline{V}_g = \underline{V}_c - \underline{V}_m \tag{1.1}$$

where $\underline{V}_g$ is the velocity-to-be-gained

$\underline{V}_m$ is the present vehicle velocity

The dynamic equation for $\underline{V}_g$ is[1]

$$\dot{\underline{V}}_g = - \underline{a}_T - Q \underline{V}_g \tag{1.2}$$

where $\underline{a}_T$ is the vehicle thrust acceleration

$$Q = \frac{\partial \underline{V}_c}{\partial \underline{r}} \qquad 3 \text{ X } 3 \text{ matrix of partials}$$

$\underline{r}$ is the present position vector

In many applications the relative contribution of the $Q \underline{V}_g$ term is small compared to $\underline{a}_T$ and may be treated as a perturbation to the solution of the problem which assumes

Q = 0. With this assumption the problem of the thesis is diagramed in two dimensional form in Figure 1.1.

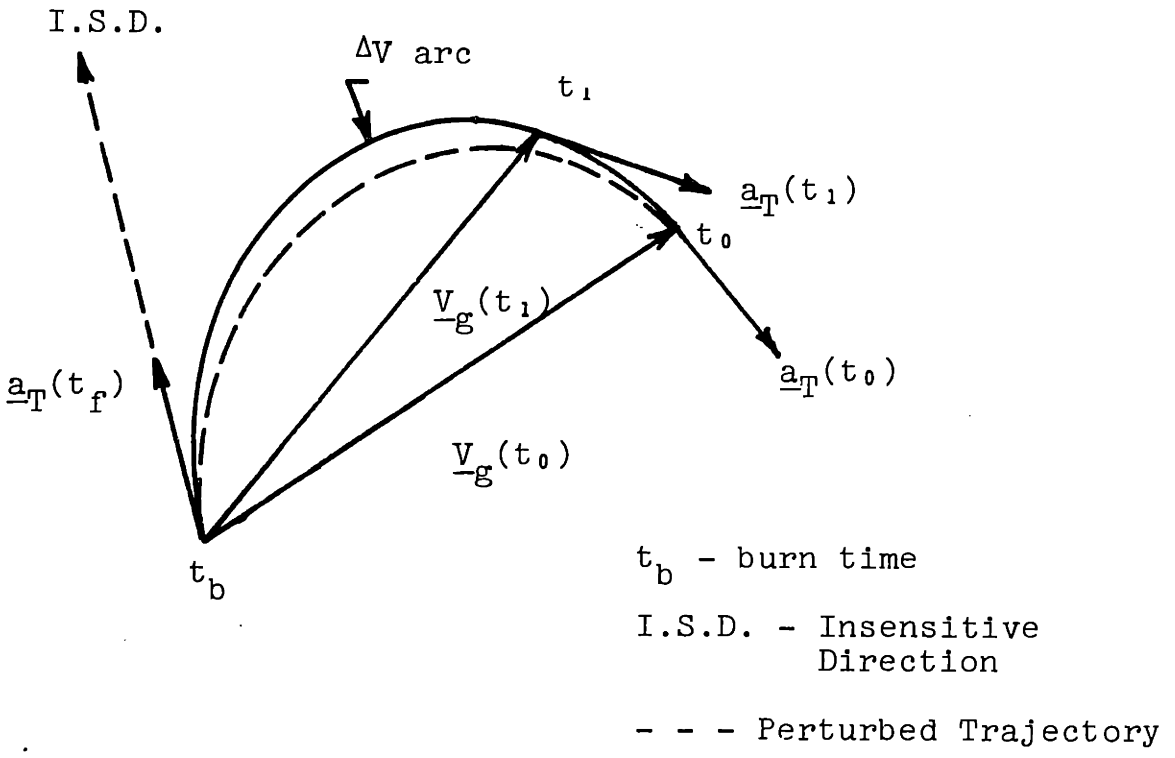

Cutoff Insensitive Guidance

Figure 1.1

Figure 1.1 is presented using only $\underline{V}_g$ as defined by Equation 1.1, thus avoiding selecting a particular $\underline{V}_c$ and $\underline{V}_m$. The problem begins at time $t = t_0$ where $\underline{V}_g = \underline{V}_{g_0}$. The ΔV to be imparted to the vehicle is represented by the ΔV arc. The

arc may be of any chosen contour but must have an arc length of ΔV and a slope which lies along the insensitive direction (I.S.D.) at the end of the burn time t_b. The commanded direction of $\underline{a}_T$ is then tangent to the ΔV arc as shown at points t_0, t_1, and t_b. The motion of the tip of the $\underline{V}_g$ vector along the V arc is a function of the thrust acceleration profile $\underline{a}_T(t)$. At $t = t_b$ the total ΔV has been expended and $\underline{a}_T$ lies parallel to the I.S.D. The shape of the ΔV contour and the magnitude of $\underline{a}_T$ then determine the angular velocity and acceleration of unit($\underline{a}_T$) in order that the desired profile be traced. The particular ΔV trajectory to be followed then imposes requirements on the vehicle autopilot and structure.

During the burn time t_b, the change in position $\underline{r}$ will introduce a perturbation in $\underline{V}_g$. In addition, thrust acceleration variances and autopilot dynamics will cause the desired ΔV trajectory to change as illustrated in Figure 1.1 by the dotted line arc. Consequently the ΔV trajectory must be periodically updated to accommodate the perturbations mentioned above.

A control scheme must be implemented which will maintain the vehicle on the commanded ΔV arc trajectory. The law could be of the form

$$\underline{\Omega}_c = k_P \, \underline{P} \times \underline{P}_c + k_I \int_0^{t_b} (\underline{P} \times \underline{P}_c) \, dt \qquad (1.5)$$

where

$$\underline{P}_c = \int_0^t \underline{\Omega}_c \, dt$$

$\underline{\Omega}_c$ - commanded vehicle angular velocity

$\underline{P}_c$ - commanded direction of unit($\underline{a}_T$)

$\underline{P}$ - present direction of ($\underline{a}_T$)

k_P - proportional steering gain

k_I - integral steering gain

$\underline{P} \times \underline{P}_c$ is the alignment error between $\underline{P}$ and $\underline{P}_c$. The proportional plus integral control of Equation 1.5 allows $\underline{P}$ to follow $\underline{P}_c$ with zero error when $\underline{\Omega}_c$ is a constant input. Proper choice of the gains k_P and k_I give the required response demanded by the ΔV curve.

In summary, the problem may be stated as

1. Expend a known ΔV along an arc of selected contour and length with a desired terminal slope.
2. Accomplish 1 by commanding $\underline{a}_T$ tangent to the arc as shown in Figure 1.1 using $\dot{\underline{V}}_g = -\underline{a}_T$.

3. Account for perturbations by periodic updating of the arc length and contour.

4. Force the vehicle to follow the commanded unit($\underline{a}_T$) direction via an appropriate control law.

1.2 Thrust Termination Control

Control laws presently in use require accurate control over the termination of powered flight. Turano[2] analyzes the cross-product methods of steering. The cross-product steering laws attempt to align $\underline{a}_T$ with $\underline{V}_g$ and may be implemented in several forms as

$$\underline{\Omega}_c = K_1 \quad \underline{a}_T \times \text{unit}(\underline{V}_g) \tag{1.3}$$

$$\underline{\Omega}_c = K_2 \quad \text{unit}(\underline{a}_T) \times \text{unit}(\underline{V}_g) \tag{1.4}$$

where $\underline{\Omega}_c$ is the commanded angular velocity k_1, k_2 are steering gains. Equations 1.3 and 1.4 command a vehicle angle rate which is proportional to the misalignment of $\underline{a}_T$ (or unit($\underline{a}_T$)) and unit($\underline{V}_g$). As $\underline{V}_g \to 0$ high angular rates are commanded as the unit($\underline{V}_g$) direction rotates to the Q $\underline{V}_g$ direction. A way to avoid this rate is to implement (see Figure 1.2)

$$\underline{\Omega}_c = k_3 \quad (-\dot{\underline{V}}_g \times \text{unit}(\underline{V}_g)) \tag{1.5}$$

where $\dot{\underline{V}}_g$ is defined by Equation 1.2

k_3 is a steering gain

Equation 1.5 maintains $-\dot{\underline{V}}_g$ aligned with $\underline{V}_g$ eliminating the rotational problem at $\underline{V}_g$ near zero.

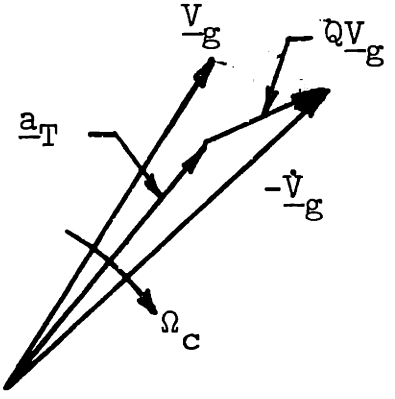

Cross Product Steering

Figure 1.2

Thrust termination is commanded when $\underline{V}_g = 0$ in Equations 1.3, 1.4 and 1.5. Good cut-off velocity accuracy may be achieved by high-speed sampling for $\underline{V}_g = 0$ and/or utilization of low level or vernier thrusting during this phase. This accuracy is required because the terminal thrust acceleration direction is nominally in a range sensitive direction.

Variations of the cross-product steering law command the thrust acceleration vector $\underline{a}_T$ to lie part way between

$\underline{V}_g$ and $-\dot{\underline{V}}_g$. Motivations for these forms might be to minimize fuel consumption or to facilitate mechanization. All of the forms of the cross-product steering law are explicit and closed-loop in nature. Perturbations in initial conditions and thrust disturbances are taken into account by periodic updating of $\underline{V}_g$.

The basic difference between the presently used cross-product steering laws and the cut-off insensitive law described in Section 1.1 is the requirement to expend the total ΔV of the rocket. The problem can be visualized as having a curved $\underline{V}_g$ instead of being defined by a straight line $(V_c - V_m)$. The unit thrust acceleration direction ($\underline{P}$) is commanded tangent to the curve. A control scheme is required to steer the vehicle thrust direction $\underline{P}$ in accordance with $\underline{P}_c$, the commanded direction.

1.3 Optimal ΔV trajectories

With a fixed amount of fuel to deplete, the problem as stated in Section 1.1 can be handled as one of specified time. An optimal ΔV trajectory over a specified burn time can be generated which satisfies the requirements. Suppose the performance index J is

$$J = \int_0^{t_b} L \, dt = \frac{1}{2} \int_0^{t_b} \Omega_c^2 \, dt \qquad (1.6)$$

where

Ω_c - commanded vehicle angular velocity

L - cost function over time t_b

t_b - burn time

Optimization of J minimizes the mean-square value of the angular velocity over the burn time. Choose a state vector

$$\underline{x} = \begin{bmatrix} V_{gx} \\ V_{gy} \\ \beta \end{bmatrix} \tag{1.7}$$

where β is the angle of thrust acceleration with respect to the x coordinate, V_{gx}, V_{gy} are the components of $\underline{V}_g$ in two dimensions.

The terminal constraints on $\underline{V}_g$ and β can be satisfied by specifying

$$\underline{\psi}\ (t_b) = \underline{x}\ (t_b) - \underline{C} = 0 \tag{1.8}$$

where

$$\underline{C} = (a,\ b,\ \beta(t_b))^T$$

$\beta(t_b)$ is specified

a, b are constant terminal tolerances for V_{gx} and V_{gy}

The necessary conditions for the solution to the problem outlined above are presented in Chapter II. The resulting trajectory for $\underline{x}(t)$ reduces $\underline{V}_g$ to zero in time t_b and commands the terminal direction of $\underline{a}_T$ by $\beta(t_b)$. In addition, the angular velocity requirements imposed on the vehicle are minimized.

Assuming for the moment the existence of the thrust termination control, the minimum time solution with hard limit on vehicle angular velocity (L = 1) is a straight line-circular arc combination for the ΔV arc as shown in Figure 1.3.

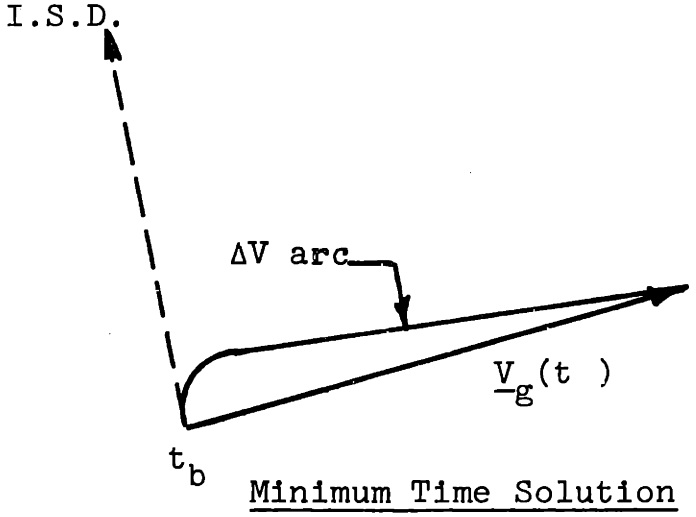

Minimum Time Solution

Figure 1.3

This trajectory reduces $\underline{V}_g$ along a straight line until a maximum rate turn is commanded to turn the thrust direction into the desired terminal direction. This solution assumes Q = 0 and $|\underline{a}_T|$ constant during the turn. Discussion of the minimum time solution is presented in Chapter II.

Optimal solutions are generally open-loop solutions which satisfy only a specified set of initial conditions, terminal constraints, and state vector and control vector time histories. Deviations in the above lead to sub-optimal or undesirable performance. The optimal trajectory solution can be developed into closed-loop control by use of perturbation feedback control. Control is done in the vicinity of the nominal path. This approach computes neighboring extremal paths[3] to an optimal trajectory. The necessity of storing state vector and control vector time histories is a distinct disadvantage. Additionally, significant computation is required to generate the nominal path. Further discussion is presented in Chapter II.

1.4 Explicit Feedback Laws

An explicit feedback technique to generate the ΔV trajectory is to fit an appropriate curve. The restrictions on the curve are that its arc length is easily computed and that the curvature may not impose excessive angular rates on the vehicle. The constraints on the trajectory are

1. Specified arc length
2. Specified final slope (I.S.D. direction)

3. Final value of (0, 0) for $\underline{V}_g$
4. Initial value of $\underline{V}_g$ given

The four constraints define uniquely a parabola arc segment. The parabola arc length is reasonable to compute. A line-circle combination may also satisfy the constraints and define an arc segment along which the thrust must be directed during the burn. As perturbations alter the ΔV trajectory, a new one is calculated. The remaining ΔV arc length and the present value of $\underline{V}_g$ are required for the update. Derivations of the ΔV trajectory generation for the parabola and the line-circular arc combination are given in Chapter III.

1.5 Additional Remarks

The computation of the insensitive direction is discussed in Chapter IV. Chapter V presents and analyzes results obtained from digital simulation.

CHAPTER II

OPTIMAL ΔV TRAJECTORY SOLUTIONS

2.1 The Minimum Time Solution

This section derives the minimum-time solution to the problem introduced in Chapter I with Q = 0 assumed. The minimum time solution implies that $\underline{V}_g$ is driven to zero as quickly as possible (final time unspecified) with the final thrust direction specified and not exceeding a maximum vehicle angular rate. Although this is not the exact specified final time problem of Chapter I, the results are educational and give insight into the specified burn time problem solution.

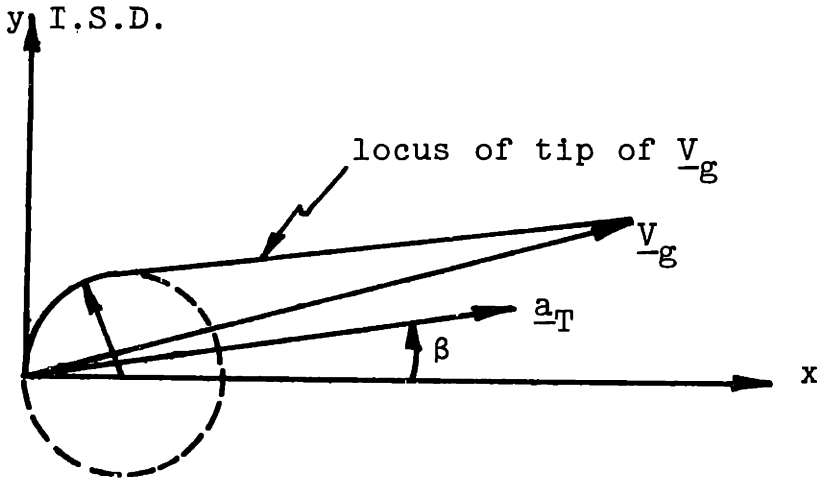

Minimum Time Solution

Figure 2.1

Assume Q = 0 in Equation 1.1. Define the state vector $\underline{x}$ as

$$\underline{x} = \begin{bmatrix} \underline{u} \\ \underline{v} \end{bmatrix}$$

where $\underline{u} = \begin{bmatrix} V_{gx} \\ V_{gy} \end{bmatrix}$ the components of $\underline{V}_g$

$$\underline{v} = \dot{\underline{u}} = \begin{bmatrix} -a_{Tx} \\ -a_{Ty} \end{bmatrix} = \begin{bmatrix} -a_T \cos\beta \\ -a_T \sin\beta \end{bmatrix}$$

Assume the control is Ω, the vehicle angular velocity and that it is bounded

$$-\Omega_{max} \leq \Omega \leq +\Omega_{max}$$

$$\Omega = \dot{\beta}$$

The system differential equations are then

$$\dot{\underline{x}} = \begin{bmatrix} \underline{v} \\ \dot{\underline{v}} \end{bmatrix} = \begin{bmatrix} \underline{v} \\ a_T \sin\beta \quad \Omega \\ -a_T \cos\beta \quad \Omega \end{bmatrix} \tag{2.1}$$

$$\dot{\underline{x}} = \begin{bmatrix} \dot{\underline{v}} \\ \Omega K \underline{v} \end{bmatrix} = \begin{bmatrix} \underline{v} \\ \underline{a} \end{bmatrix}$$

where

$$K = \begin{bmatrix} 0 & -1 \\ 1 & 0 \end{bmatrix}$$

For minimum time problems the cost L = 1. Thus, the Hamiltonian is written as

$$H = 1 + \underline{\mu}^T \underline{v} + \underline{\gamma}^T K \underline{v} \tag{2.2}$$

where μ and $\underline{\gamma}$ are the costate vectors for $\underline{u}$ and $\underline{v}$ respectively.

A necessary condition for optimality is

$$\frac{\partial H}{\partial \Omega} = \underline{\gamma}^T K \underline{v} = 0 \tag{2.3}$$

Since the control appears linearly in the Hamiltonian, Equation 2.3 does not determine the optimal control and may be determined by a singular arc. The Pontryagin minimum principle[3] may be applied to Equation 2.2 to determine the optimal control Ω. $\underline{\gamma}^T K \underline{v}$ acts as a switch function and determines the sign of Ω. Ω is then defined as

$$\begin{aligned} &\text{If } \underline{\gamma}^T > K \underline{v}, \ \Omega = -\Omega_{max} \\ &\underline{\gamma}^T > K \underline{v}, \ \Omega = +\Omega_{max} \end{aligned} \tag{2.4}$$

Equation 2.4 defines Ω as the optimal control since it minimizes H over the set of all possible controls Ω.

If $\underline{\gamma}^T K \underline{v} = 0$, the control Ω may be determined by the requirement that the time derivates of H_Ω be equal to zero. Differentiating 2.3 with respect to time

$$\dot{H}_\Omega = \dot{\underline{\gamma}}^T K \underline{v} + \underline{\gamma}^T K \underline{a} \tag{2.5}$$

A necessary condition on the costate vector γ for optimality is

$$\dot{\gamma} = - \frac{\partial H}{\partial \underline{v}} = - \underline{\mu}^T - \underline{\gamma}^T K \underline{v} \tag{2.6}$$

Using 2.6 in 2.5, and $\underline{a} = \Omega K \underline{v}$

$$\dot{H}_\Omega = - \underline{\mu}^T K \underline{v} - \underline{\gamma}^T K^2 \underline{v} \Omega + \underline{\gamma}^T K^2 \Omega \tag{2.7a}$$

$$\dot{H}_\Omega = -\underline{\mu}^T K \underline{v} = 0 \tag{2.7b}$$

Equation 2.7b does not determine Ω and 2.3 must be differentiated again.

$$\ddot{H}_\Omega = - \dot{\underline{\mu}}^T K \underline{v} - \underline{\mu}^T K \underline{a} \tag{2.8}$$

The necessary condition on the costate vector $\underline{\mu}$ is

$$\dot{\underline{\mu}}^T = - \frac{\partial H}{\partial \underline{v}} = 0 \tag{2.9}$$

From 2.7b and 2.9 and

$$\underline{\mu}^T K \underline{v} = \underline{\mu}^T K \underline{a} = 0 \qquad (2.10a)$$

or

$$\underline{\mu}^T K \underline{v} = \Omega \underline{\mu}^T K^2 \underline{v} = 0 \qquad (2.10b)$$

Define

$$\underline{v}_\perp = K \underline{v} = \begin{bmatrix} 0 & -1 \\ 1 & 0 \end{bmatrix} \underline{v} \qquad (2.11)$$

Note that $K \underline{v} = - \underline{v}$. Then 2.10b with $\underline{\gamma}^T K \underline{v} = 0$ becomes

$$\underline{\gamma}^T \underline{v}_\perp = \underline{\mu}^T \underline{v}_\perp = - \Omega \underline{\mu}^T \underline{v} = 0 \qquad (2.12)$$

Equation 2.12 determines that the optimal $\Omega = 0$ since $\underline{v}$ and $\underline{v}_\perp$ are orthogonal vectors. The above results define the commanded angular velocity $\underline{\Omega}$ to be zero when $\underline{v}$ and the costate vectors $\underline{\mu}$ and $\underline{\gamma}$ are collinear. When the vectors are not collinear, Ω is commanded as specified by 2.4. See Figure 2.2.

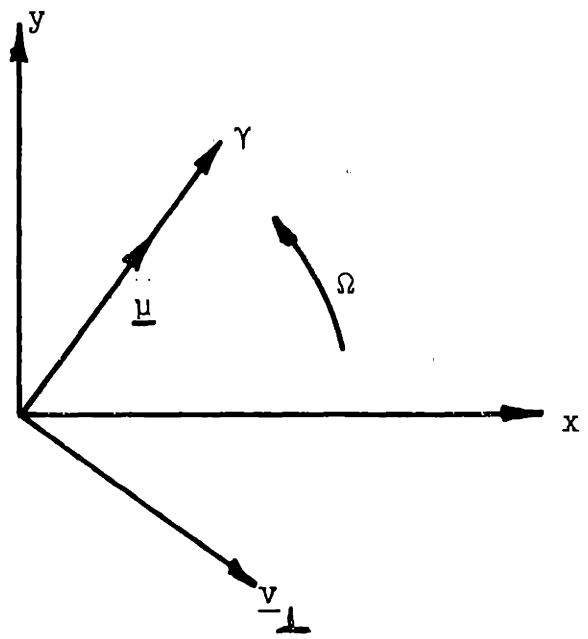

Costate Vectors - Minimum Time Solution

Figure 2.2

The minimum time solution using a bounded angular velocity as the control specifies Ω to be either zero or at its positive or negative maximum values. In $\underline{V}_g$ space the curve is a straight line or a circular arc as shown in Figure 2.1 when Q is assumed equal to zero and $|\underline{a}_T|$ is constant.

If Q is not assumed to be a null matrix

$$\dot{\underline{V}}_g = - \underline{a}_T - Q \underline{V}_g \qquad (2.13)$$

Assume $\frac{d}{dt}(Q\ \underline{V}_g) \simeq 0$

Then

$$\underline{u} = \underline{V}_g$$

$$\underline{v} = \dot{\underline{u}} = -\underline{a}_T - \underline{Q}\ \underline{u} \tag{2.14}$$

$$\underline{x} = \begin{bmatrix} \underline{u} \\ \underline{v} \end{bmatrix} \tag{2.15}$$

$$\dot{\underline{u}} = -\underline{a}_T - Q\ \underline{u} \tag{2.16a}$$

$$\dot{\underline{v}} = \underline{a}_r = \Omega\ \underline{K}\ \underline{v} = \Omega\ K\ (-\underline{a}_T - Q\ \underline{u}) \tag{2.16b}$$

The Hamiltonian is then written as

$$H = 1 + \underline{\mu}^T\ (-a_T - Q\ \underline{u}) + \underline{\gamma}^T(-\Omega\ K\underline{a}_T - \Omega\ K\ Q\ \underline{u}) \tag{2.17}$$

The differential equation for the costate is

$$\dot{\underline{\mu}}^T = -\frac{\partial H}{\partial \underline{u}} = (-\underline{\mu}^T - \underline{\gamma}^T\ K\Omega)\ Q \tag{2.18}$$

With Q nonzero, $\underline{\mu}$ is not a constant vector. The effect of the $(Q\ \underline{V}_g)$ term can be treated as a perturbation

of the costate vector $\underline{\mu}$. In $\underline{V}_g$ space the $(Q\ \underline{V}_g)$ term is a perturbation of the ΔV trajectory solution which assumes $Q = 0$.

2.2 Final Time Specified

The requirement of expending a prescribed amount of fuel and the assumption that the rocket motor is not throttable, allows the problem to be handled as one of final time specified (t_f). The state vector can be written in a different form from Section 2.1 as

$$\underline{x} = \begin{bmatrix} V_{gx} \\ V_{gy} \\ \beta \end{bmatrix} \tag{2.19}$$

where β is the angle of the thrust acceleration from the x axis. (Refer to Figure 2.3.) The differential equation for the state in this form is

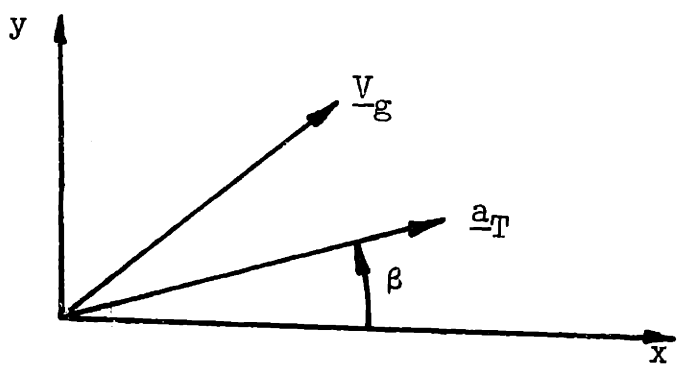

Figure 2.3
Optimal Specified Burn Time Problem

$$\dot{\underline{x}} = \begin{bmatrix} -a_T \cos\beta \\ -a_T \sin\beta \\ \Omega \end{bmatrix} = \underline{f}(x) \qquad (2.20)$$

A performance index J is chosen to minimize the mean-square of the vehicle angular velocity over the burn time

$$J = \frac{1}{2}\int_0^{t_f} \Omega^2 \, dt \qquad (2.21)$$

Using 2.21, the Hamiltonian of the system is written as

$$H = \frac{1}{2} \Omega^2 + \underline{\lambda}^T \underline{f} \qquad (2.22)$$

where $\underline{\lambda}$ is the costate vector or Lagrange multiplier.

The necessary conditions for J to have a stationary value are:

$$\dot{\underline{\lambda}} = - \left(\frac{\partial \underline{f}}{\partial \underline{x}}\right)^T \underline{\lambda} - \left(\frac{\partial L}{\partial \underline{x}}\right)^T \qquad (2.23a)$$

$$\frac{\partial H}{\partial \Omega} = \frac{\partial \underline{f}}{\partial \Omega} \underline{\lambda} + \frac{\partial L}{\partial \Omega} = 0 \qquad (2.23b)$$

Initial condition $\underline{x}(0)$ - given (2.23c)

Terminal constraints of state vector

$$\underline{\psi}\ (\underline{x}(t_f)) = (x_1 - a,\ x_2 - b,\ x_3 - c) = 0 \qquad (2.23d)$$

where a, b are constant tolerances and $c = \beta(t_f)$.

$$\underline{\lambda}(t_f) = \underline{\gamma}^T \frac{\partial \underline{\psi}}{\partial x} = \underline{\gamma}^T \qquad (2.23e)$$

The necessary conditions stated in 2.23 form a two-point boundary value problem. The optimal control history of $\Omega(t)$ can be solved for using a technique such as the steepest descent method. A program using the gradient projection method[5] was developed to solve the problem stated above. The gradient projection method is described in Appendix A. It was used as a comparison with the performance of the explicit guidance laws which were developed and are presented in Chapter III. The primary goal of this formulation was to maintain the vehicle rates as low as possible while satisfying the terminal constraints of $\underline{V}_g\ (t_f) = \underline{0}$ and $\beta(t_f)$ specified.

2.3 Perturbation Feedback Control

The solution to the two-point boundary problem presented in Section 2.2 generates an open-loop control history for $\Omega(t)$ which applies only to a particular set of initial conditions, nominal acceleration profile and terminal constraints. Perturbations to the above will result in a sub-optimal performance. It is desirable to have a closed-loop control law which is insensitive to the presence of these anomalies. This section outlines a scheme using neighboring external paths.[3]

Suppose a control function $\Omega(t)$ which satisfies the problem stated in Section 2.2 has been determined. Along with $\Omega(t)$, there are corresponding time histories $\underline{x}(t)$ and $\underline{\lambda}(t)$. Consider small perturbations from the extremal path produced by small perturbations in the initial state $\delta\underline{x}_0$ and in the terminal conditions $\delta\psi$. These perturbations give rise to perturbations $\delta\underline{x}(t)$, $\delta\underline{\lambda}(t)$, $\delta\Omega(t)$, and $\delta\underline{\lambda}$ on the basis of linearizing around the extremal path. The perturbations are

$$\delta\underline{\dot{x}} = \underline{f}_x \quad \delta\underline{x} + \underline{f}_\Omega \, \delta\Omega \tag{2.24}$$

$$\delta\underline{\dot{\lambda}} = - H_{xx} \quad \delta\underline{x} - \underline{f}_x^T \quad \delta\lambda - H_{x\Omega} \, \delta\Omega \tag{2.25}$$

$$0 = -H_{\Omega x} \quad \delta \underline{x} - (\delta \underline{\lambda}^{T} \underline{f}_{\Omega})^{T} - H_{\Omega\Omega} \delta\Omega \tag{2.26}$$

$$0 = H_{\Omega x} \quad \delta x + \underline{f}_{\Omega}^{T} \delta \underline{\lambda} + H_{\Omega\Omega} \delta\Omega \tag{2.27}$$

$\delta \underline{x}_0$ specified

$$\delta \underline{\lambda}(t_f) = \left[\underline{\gamma}^{T} \underline{\psi}_{xx} \delta \underline{x} + \underline{\psi}_{x}^{T} \, d\underline{\gamma} \right]_{t=t_f} \tag{2.28}$$

$$\delta \underline{\psi} = [\underline{\psi}_{\underline{x}} \quad \delta_{\underline{x}}]_{t=t_f} \tag{2.29}$$

An augmented performance index $\bar{J}$ may be written from 2.21 as

$$\bar{J} = \underline{\lambda}^{T} \underline{\psi}(t_f) + \int_0^{t_f} (H - \underline{\lambda}^{T} \dot{\underline{x}}) \, dt \tag{2.30}$$

where

$$H = L + \underline{\lambda}^{T} \underline{f} = \frac{1}{2} \Omega^2 + \underline{\lambda}^{T} \underline{f}$$

and $\underline{\lambda}^{T}$ is the Lagrange multiplier for the final value of constraint $\underline{\psi}(t_f)$. Consider expansion of the performance index J and constraints to second order (since all first order terms vanish about a trajectory satisfying 2.20, 2.21, 2.22 and 2.23). This may be accomplished by expanding the

augmented criterion $\bar{J}$ of 2.30 to second order and all constraints to first order.[3] This leads to

$$\delta^2 \bar{J} = \left(\frac{1}{2} \delta \underline{x}^T \quad \underline{\gamma}^T \psi_{xx} \delta \underline{x} \right)_{t=t_f}$$

$$+ \frac{1}{2} \int_0^{t_f} \left[\delta \underline{x}^T \quad \Omega \right] \begin{bmatrix} H_{xx} & H_{x\Omega} \\ H_{\Omega x} & H_{\Omega\Omega} \end{bmatrix} \begin{bmatrix} \delta \underline{x} \\ \Omega \end{bmatrix} dt \qquad (2.31)$$

Subject to

$$\delta \dot{\underline{x}} = \underline{f}_x \, \delta \underline{x} + \underline{f}_\Omega \, \delta\Omega \qquad (2.32)$$

$$\delta \underline{x}_0 \text{ specified} \qquad (2.33)$$

$$\delta \underline{\psi} = \left(\underline{\psi}_x \quad \delta_x \right)_{t=t_f} \qquad (2.34)$$

where $\delta \underline{\psi}$ is specified

A neighboring extremal path is determined by evaluating $\delta\Omega$ such that $\delta^2 \bar{J}$ is minimized subject to 2.32 through 2.34. It is now clear that equations 2.24 through 2.29 represent a linear two point boundary-value problem since the coefficients are evaluated on the extremal path. Equation 2.27 can be solved for $\delta\Omega$ provided $H_{\Omega\Omega}$ is nonsingular for $0 \leq t \leq t_f$.

$$\delta\Omega = - H_{\Omega\Omega}^{-1}(H_{\Omega x}\ \delta\underline{x} + \underline{f}_{\Omega}^{T}\ \delta\underline{\lambda}) \qquad (2.35)$$

Equation 2.35 may be put in the form [3]

$$\delta\Omega = - K_1\ (t)\ \delta\underline{x} - K_2\ (t)\ \delta\underline{\psi} \qquad (2.36)$$

Equation 2.36 may be regarded as a neighboring optimum feedback law since it will produce desired small changes in the terminal condition $\underline{\delta\psi}$ while minimizing the performance index J of 2.21.

The method of neighboring extremals carries the distinct disadvantage of having large storage requirements. Nominal time histories of state and control vectors are required in addition to the storage of the gain matrices $K_1(t)$ and $K_2(t)$ of 2.36. Substantial calculations are also required to generate the nominal profiles. For these reasons this method was not pursued further in this thesis.

CHAPTER III

EXPLICIT CLOSED-LOOP GUIDANCE LAWS

3.1 Introduction

The discussions of Chapters I and II point out the desirability of the control law being explicit and closed-loop in nature. Perturbations in initial and final conditions, variances in thrust acceleration, and autopilot dynamics are the basic considerations. In addition, there are requirements for mathematical simplicity and reasonable computer storage needs.

Since the rocket motor is assumed to have no cut-off mechanism, the expendable fuel on board must be burned off. The energy transfer imparts a delta velocity (ΔV) change to the vehicle. If the ΔV occurs in a carefully controlled manner, $\underline{V}_g$ can be reduced to zero in the burn time and the terminal direction of $\underline{a}_T$ can lie in a preferred direction. The uncertainties in burn time and burn rate appear as a velocity error. The velocity error is directed in the terminal insensitive direction if conservative estimates are used in the vehicle energy model.

A direct method of controlling the nature of the ΔV curve is to fit it to a curve. This curve would then have a known

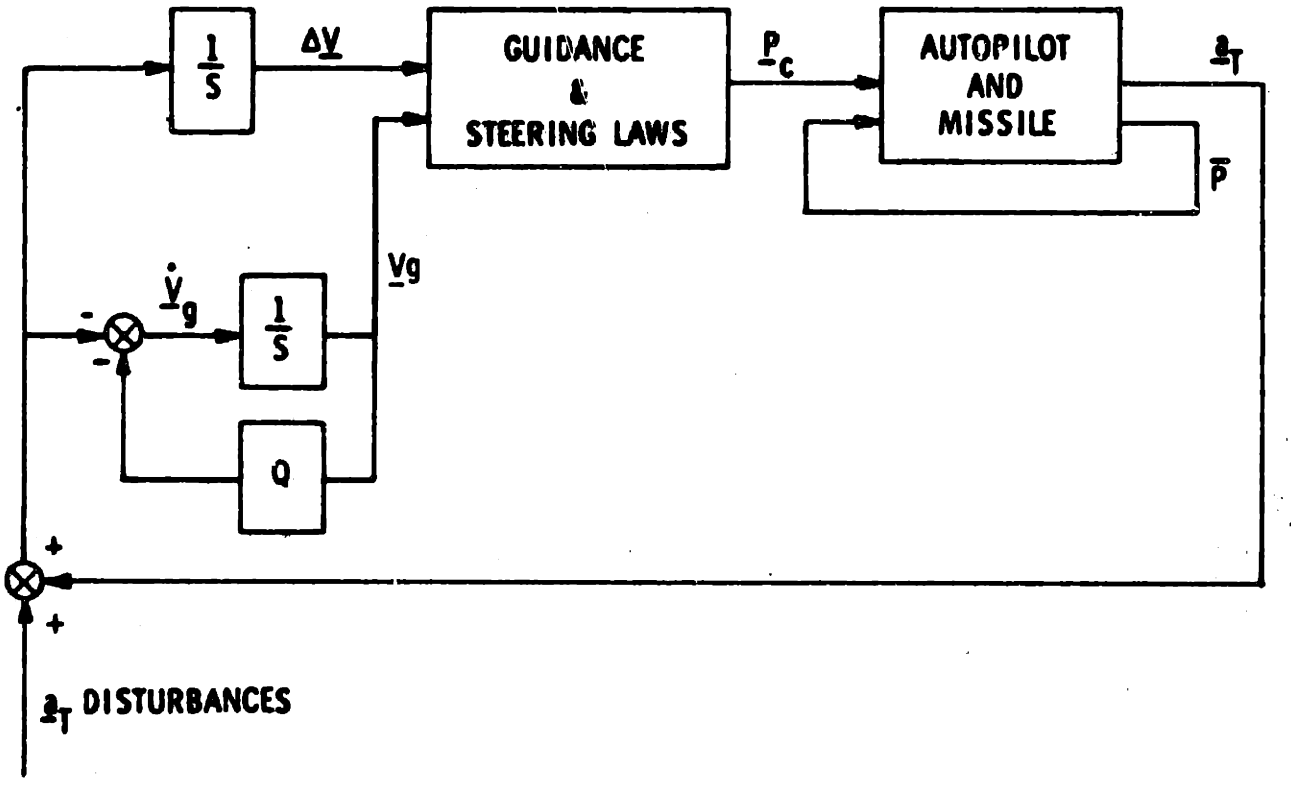

Fig. 3-1 System block diagram.

initial value ($\underline{V}_g(0)$), a final value of zero, a desired final slope, and an arc length equal to ΔV. Figure 3.1 shows the system block diagram. The guidance law uses $\Delta\underline{V}$ and $\underline{V}_g$ information to compute the ΔV trajectory in order to obtain the commanded thrust direction $\underline{P}_c$. The function of the autopilot is to generate commands based on the attitude error between $\underline{P}_c$ and $\underline{P}$. The missile section represents vehicle dynamics. The thrust acceleration $\underline{a}_T$ is fed back and is used to update both $\underline{V}_g$ and the ΔV trajectory. Here the $Q\ \underline{V}_g$ term of $\dot{\underline{V}}_g$ is treated as a perturbation. ΔV uncertainty and thrust and autopilot disturbances are also shown.

Two types of curves were considered based primarily on ease of computation of arc length. The curves are the parabola and the straight line-circular arc combination. Derivations associated with these profiles are presented in the next two sections.

3.2 Parabola Guidance

The general conic equation can be written as

$$A\,x^2 + Bxy + Cy^2 + Dx + Ey + F = 0 \qquad (3.1)$$

Divide (3.1) by A

$$x^2 + B'xy + C'y^2 + D'x + E'y + F' = 0 \qquad (3.2)$$

Equation 3.2 has five coefficients allowing five constraints to determine the curve. Refer to Figure 3.2 for the following discussion. If the final point is chosen as (0, 0) then F = 0. Equation 3.2 represents a parabola if the first three terms are a perfect square. (Drop prime notation.)

$$(x \pm 2\sqrt{C}\, y)^2 + Dx + Ey = 0 \tag{3.3}$$

$$B^2 = 4\,C,\quad B = \pm 2\sqrt{C}$$

Change the nomenclature

$$(x + ay)^2 + by + cx = 0 \tag{3.4}$$

At (0, 0) the slope is m2

$$\frac{dy}{dx} = \frac{-c}{b} = m2 \tag{3.5}$$

At initial point (x_1, y_1), solve for b

$$b = \frac{(x_1 + a\, y_1)^2}{(y_1 - m_2 x_1)} \tag{3.6}$$

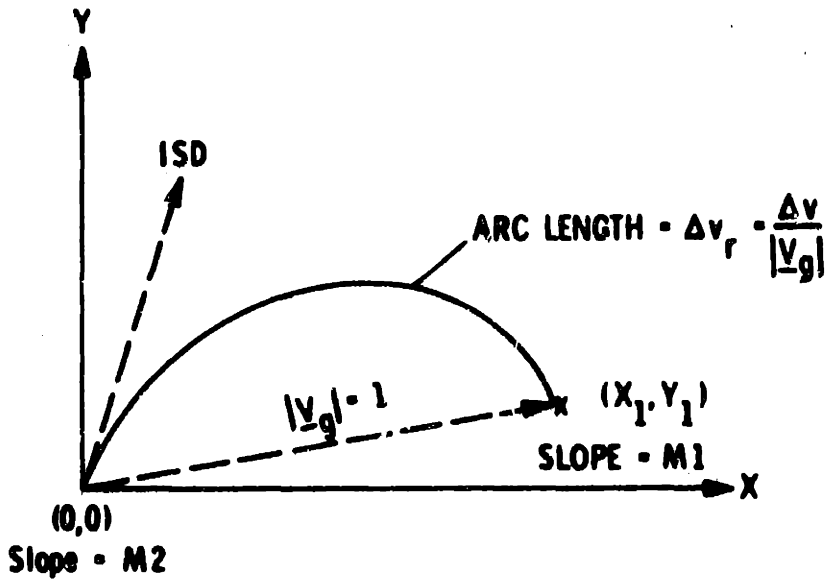

Fig. 3-2 Parabola guidance.

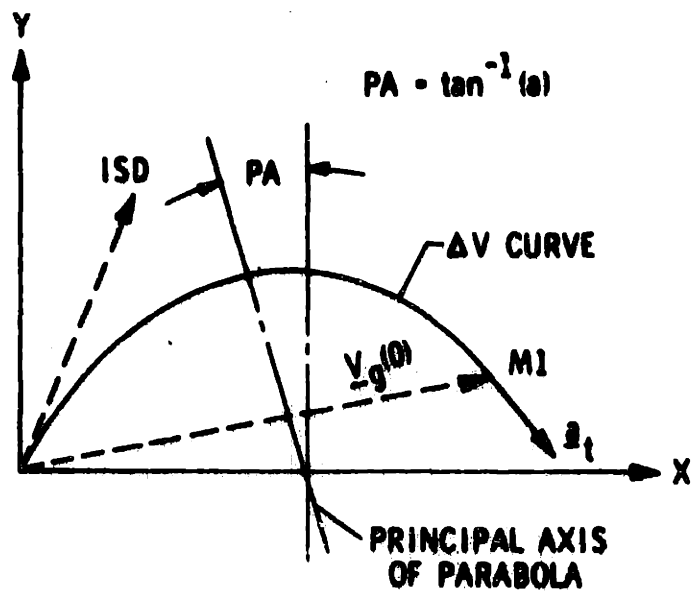

Fig. 3-3 Parabola orientation.

'a' is the last coefficient to be determined. It is uniquely defined by the arc length constraint. 'a' will be computed using an iterative procedure.

1. Guess a, arc length S given
2. Solve for b using 3.6 and c using 3.5
3. Solve for the slope at the initial point m1

$$m1 = -\frac{(2x_1 + 2\,a\,y_1 + c)}{(2\,a\,x_1 + 2\,a^2\,y_1 + b)} \tag{3.7}$$

4. The coefficient 'a' is the tangent of the angle between the y axis and the principal axis of the parabola as shown in Figure 3.3. Rotate the slopes m1 and m2 into the coordinate frame parallel to the principal axis

$$m3 = (m1 - a)/(1 + m1\,a)$$
$$m4 = (m2 - a)/(1 + m2\,a) \tag{3.8}$$

5. Compute the parameter of the parabola

$$P = (b - ac)/(1 + a^2)^{3/2} \tag{3.9}$$

where P is invariant

6. Compute the arc length of the parabola

$$S_e = \int_{m3}^{m4} dS_e = \int_{m3}^{m4} \frac{P}{2}\,(1 + y'^2)^{1/2}\,dy' \tag{3.10}$$

where

$$y' = dy/dx \tag{3.11}$$

then

$$S_e = \frac{P}{4}\left[m4(1 + m4^2)^{1/2} + \log\left(m4 + (1 + m4^2)^{1/2}\right)\right. \\ \left. - m3\,(1 + m3^2)^{1/2} - \log\left(m3 + (1 + m3^2)^{1/2}\right)\right] \tag{3.12}$$

7. The error in arc length is

$$Err_s = S_e - S \tag{3.13}$$

8. Compute a numerical derivate $\Delta S/\Delta a$ where $\Delta S = S_{\Delta a} - S_e$

$$S_{\Delta a} = S(a \pm \Delta a)$$

Δa = numerically appropriate constant (approximately 10^{-4})

9. Update 'a' by

$$a_{new} = a_{old} - Err_s \,/\, (\Delta S/\Delta a) \tag{3.14}$$

10. Repeat starting at 2 until arc length error is less than a prescribed amount.

The method outlined above rotates the principal axis of the parabola and adjusts the shape (parameter) until the arc length constraint is satisfied. With a reasonable initial guess of 'a' the coefficients of the parabola should be found in a few iterations. Subsequent updates of the coefficients would use the last solution value for 'a'. Perturbations from the desired parabola will cause the coefficients to change requiring a periodic update. The desired direction of the thrust acceleration is tangent to the arc as shown in Figure 3.3. The value of this slope is m1 from Equation 3.7. The rate of change along the ΔV trajectory is of course the thrust acceleration. The vehicle angular velocity and acceleration required is that needed to keep $\underline{a}_T$ tangent to the curve. The angular velocity Ω of the vehicle is then a function of the curvature and the thrust acceleration at a particular point on the parabola. This function is

$$\Omega = a_T/\text{RADCURV} \tag{3.14}$$

where RADCURV is the radius of curvature

$$a_T = |\underline{a}_T|$$

The ΔV trajectories for $\Delta V/|\Delta \underline{V}_g(0)| = \Delta V_r$ ratios of 1.1, 1.3, and 1.5 are shown in Figures 3.4, 3.5 and 3.6. The desired terminal direction in all cases is along the positive vertical axis.* The initial $\underline{V}_g$ positions were chosen at various angles at a radius of 1 from the final (0, 0) condition for $\underline{V}_g$. Comparing identical starting positions for the different ΔV_r ratios leads to the obvious conclusion that the more excess fuel available to waste in the turn, the slower the turning rate allowed. Looking at Figure 3.4, for example, as the initial $\underline{V}_g$ position is swung toward the final desired thrust direction, the required vehicle rates become lower. At the higher ΔV_r ratios, and as the initial position swings counter-clockwise, the vertex of the desired parabola moves toward the initial $\underline{V}_g$ position. As is expected, as the initial point moves clockwise away from the terminal thrust direction, the curvature of the parabola becomes more severe.

If one assumes that the horizontal axis of Figure 3.3 represents the down range direction, the initial $\underline{V}_g$ positions which allow lower vehicle rates, incur larger penalties in terms of range capability. Thus the longer the range required, the less energy available for the turn, which implies higher vehicle rates near thrust termination.

---

*The T.S.D. is an arbitrary direction however.

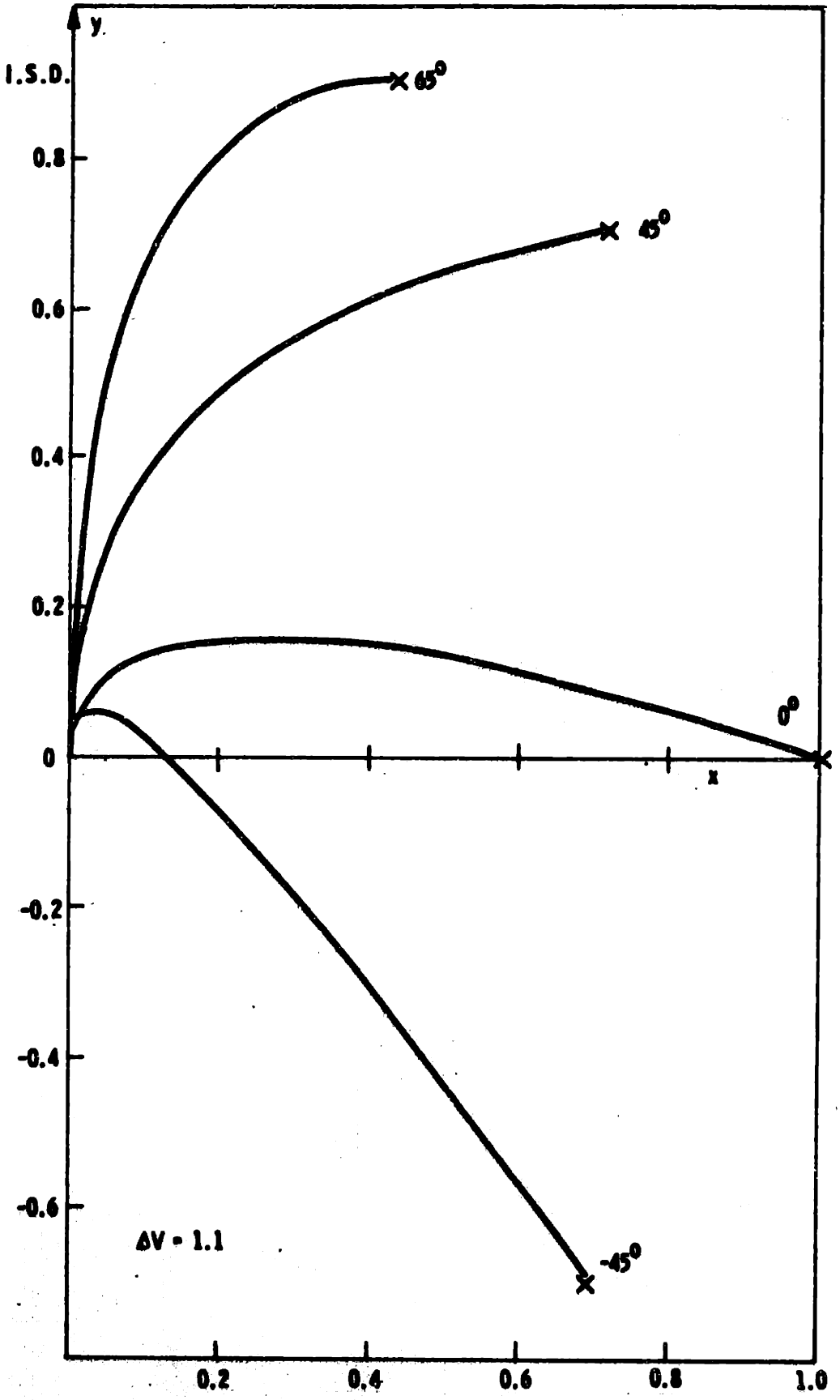

Fig. 3-4 Parabolic trajectories ($\Delta V_r = 1.1$).

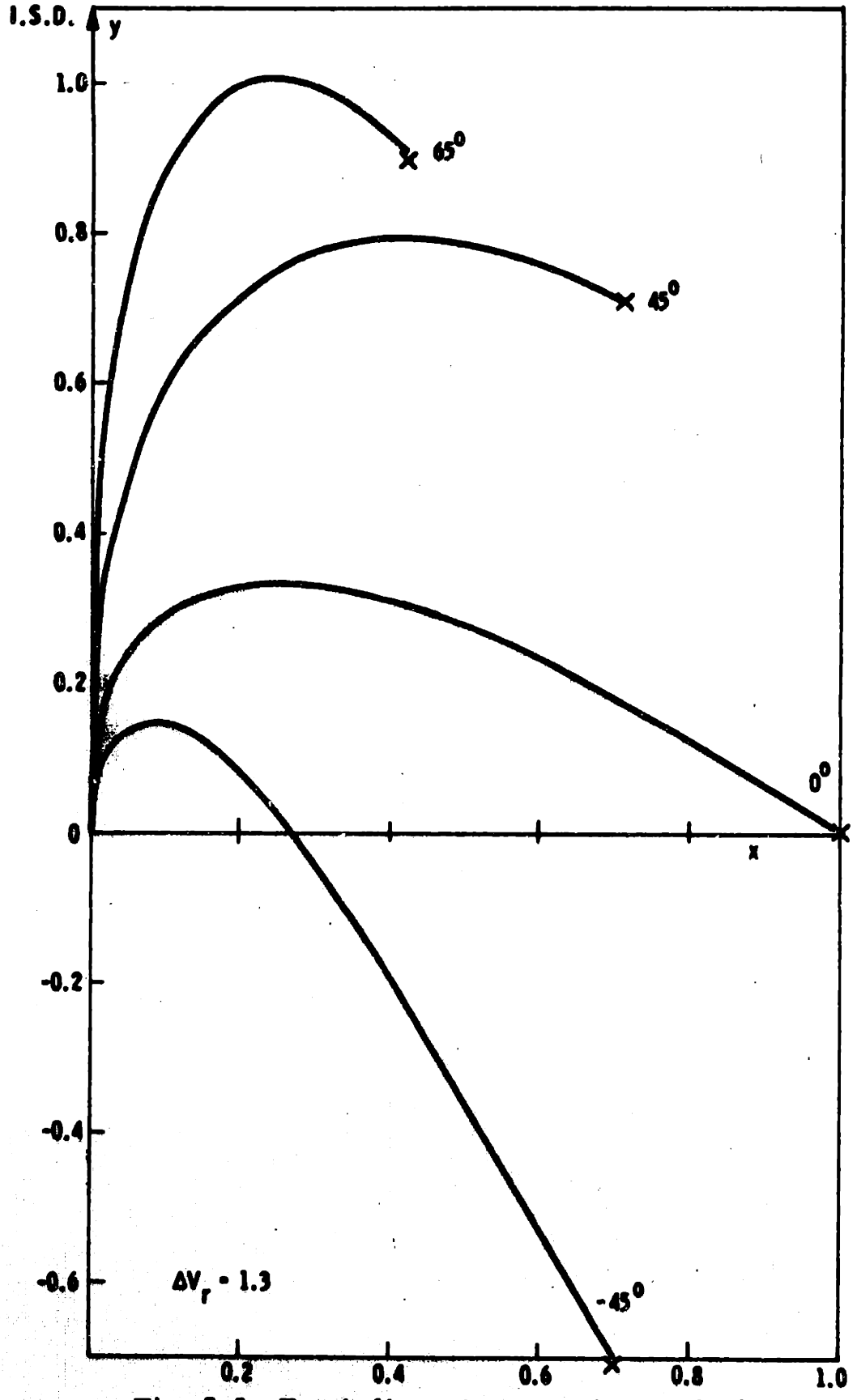

Fig. 3-5 Parabolic trajectories ($\Delta V_r = 1.3$).

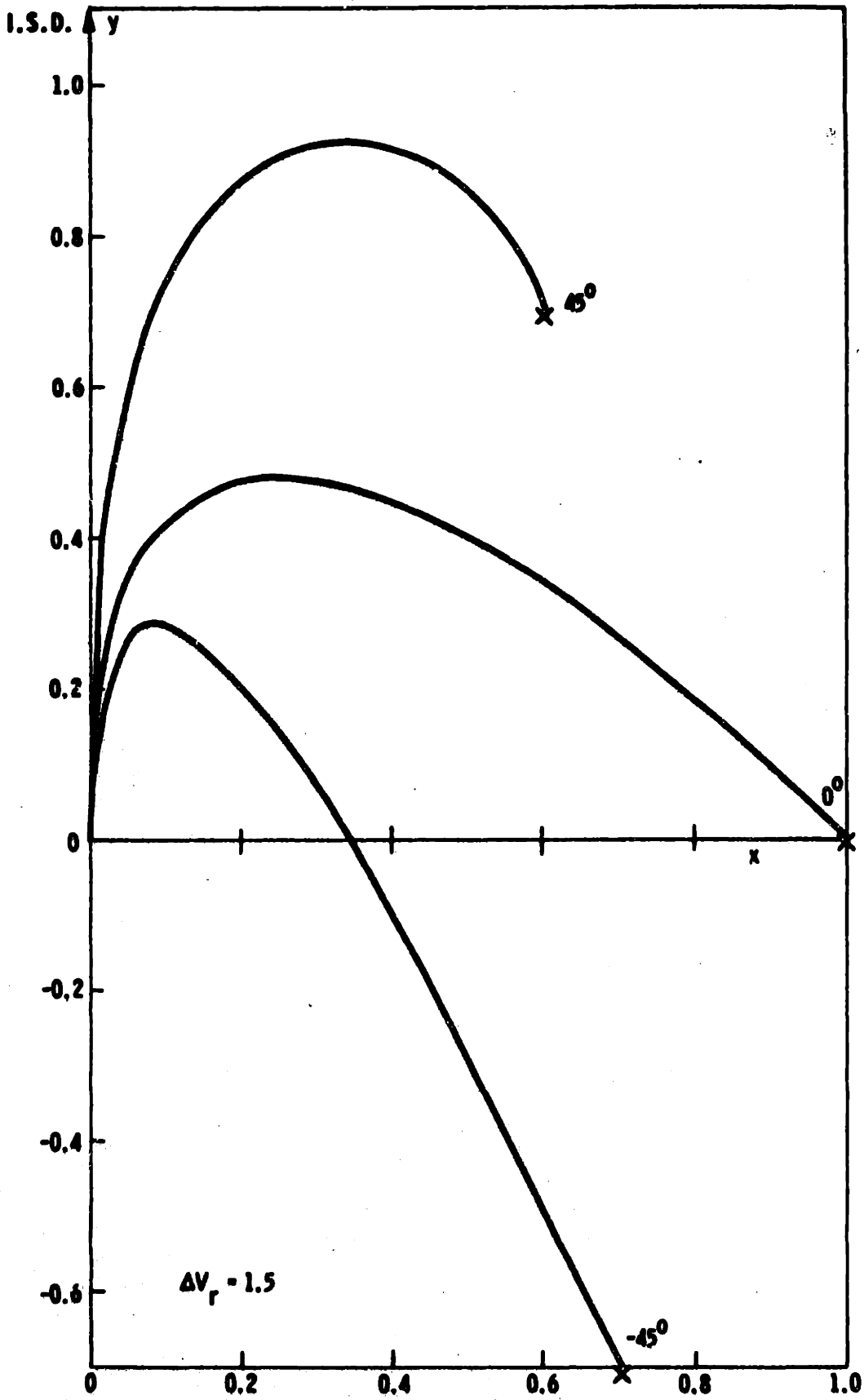

Fig. 3-6 Parabolic trajectories ($\Delta V_r = 1.5$).

An estimate of the required vehicle rates can be made with knowledge of the thrust acceleration. The thrust acceleration may be modeled using reasonable values of M_i/M_f and T_i/T_f where M_i/M_f is the initial to final mass ratio and T_i/T_f is the initial to final thrust force ratio. Constant mass flow rate will be assumed.

Let the thrust acceleration be modeled as

$$a_T = \frac{T_i + \dot{T}\, t}{M_i + \dot{M}\, t} \tag{3.15}$$

where $\dot{T}$ is the thrust force rate of change and $\dot{M}$ is the mass flow rate. With the model of 3.15, control of the engine exhaust velocity or specific impulse is assumed.

Since $$\dot{M} = \frac{M_f - M_i}{t_B} \quad , \quad \dot{T} = \frac{T_f - T_i}{t_B}$$

$$a_T = \frac{T_i}{M_i} \frac{\left(1 + \left(\frac{T_f - T_i}{T_i}\right)\left(\frac{t}{t_B}\right)\right)}{\left(1 + \left(\frac{M_f - M_i}{M_i}\right)\left(\frac{t}{t_B}\right)\right)} \tag{3.16}$$

or

$$a_T = \frac{T_i}{M_i} \frac{\left(1 - \left(1 - \frac{T_f}{T_i}\right)\left(\frac{t}{t_B}\right)\right)}{\left(1 - \left(1 - \frac{M_f}{M_i}\right)\left(\frac{t}{t_B}\right)\right)} \tag{3.17}$$

Let

$$T = T_i/T_f \tag{3.18}$$

$$R = M_i/M_f \tag{3.19}$$

$$K_a = T_i/M_i$$

Then

$$a_T = K_a \frac{1-[(T-1)/T](t/t_b)}{1-[(R-1)/R](t/t_b)} \tag{3.20}$$

K_a may be calculated by use of the ΔV and integrating 3.20 from $t = 0$ to $t = t_b$. Let $\frac{t}{t_b} = \tau$. Then $dt = t_b\, d\tau$.

Integrating 3.20 using τ from 0 to 1 results in

$$\Delta V = K_a \left[\frac{R(T-1)}{T(R-1)} + \frac{\left(\frac{T-1}{T} - \frac{R-1}{R}\right) \log(1/R)}{\left(\frac{R-1}{R}\right)^2} \right] t_b \tag{3.21}$$

Therefore K_a is determined by

$$K_a = \frac{\Delta V}{[\,]t_b} \tag{3.22}$$

Using 3.22 in 3.20 and dividing by $|\underline{V}_g|$

$$\frac{a_T\, t_b}{|\underline{V}_g|} = \frac{\Delta V_r}{[\quad]} \left\{ \frac{1 - \left|\frac{T-1}{T}\right|^{\tau}}{1 - \left|\frac{R-1}{T}\right|^{\tau}} \right\} \tag{3.23}$$

Define $\frac{a_T\, t_b}{|\underline{V}_g|}$ as the normalized a_T or a_T norm

Normalized a_T profiles are shown in Figures 3.7, 3.8 and 3.9 for a mass ratio of 3 and 6 and thrust force ratios of 1.0, .5 and 1.5.

With the estimate of a_T, the calculation of the required Ω can be made. One can approach the design problem by starting with the nominal value of $|\underline{V}_g|$ to be encountered. Then the effects of different values of ΔV_r can be examined. The angular velocity Ω can be calculated using 3.23 and the expression for the radius of curvature at a point on the curve

$$\text{RADCURV} = \frac{(1 + y'^2)^{3/2}}{y''} \tag{3.24}$$

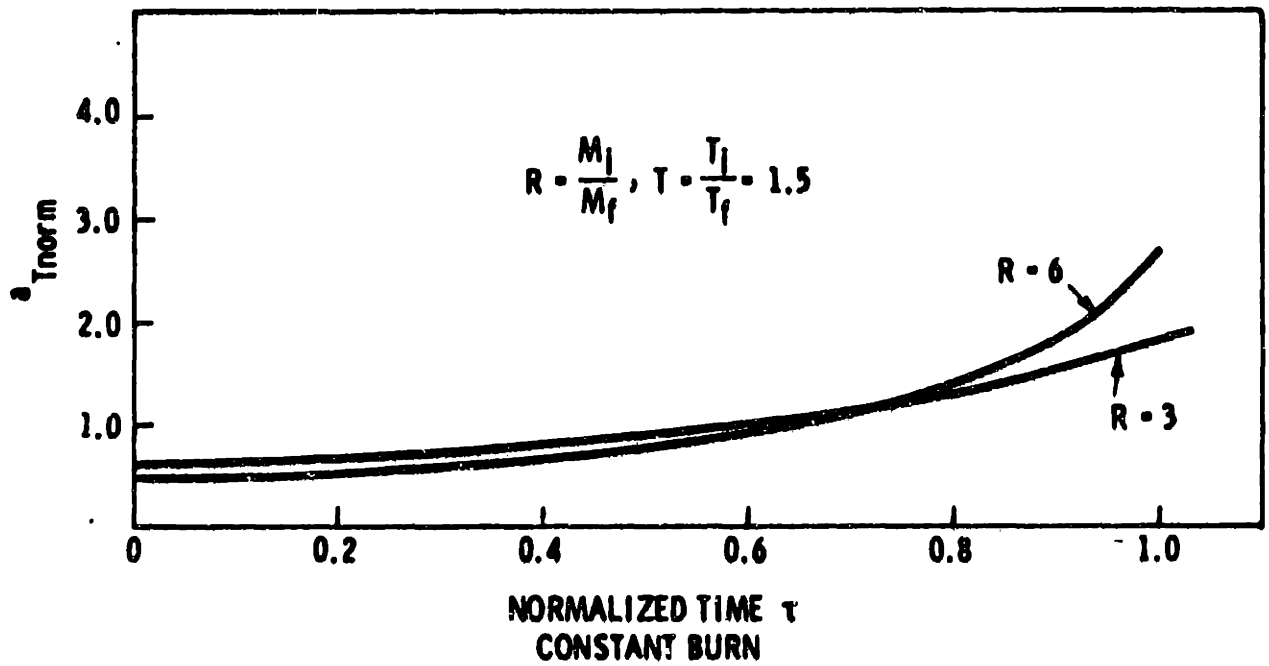

Fig. 3-7 Normalized a_t vs normalized time τ.

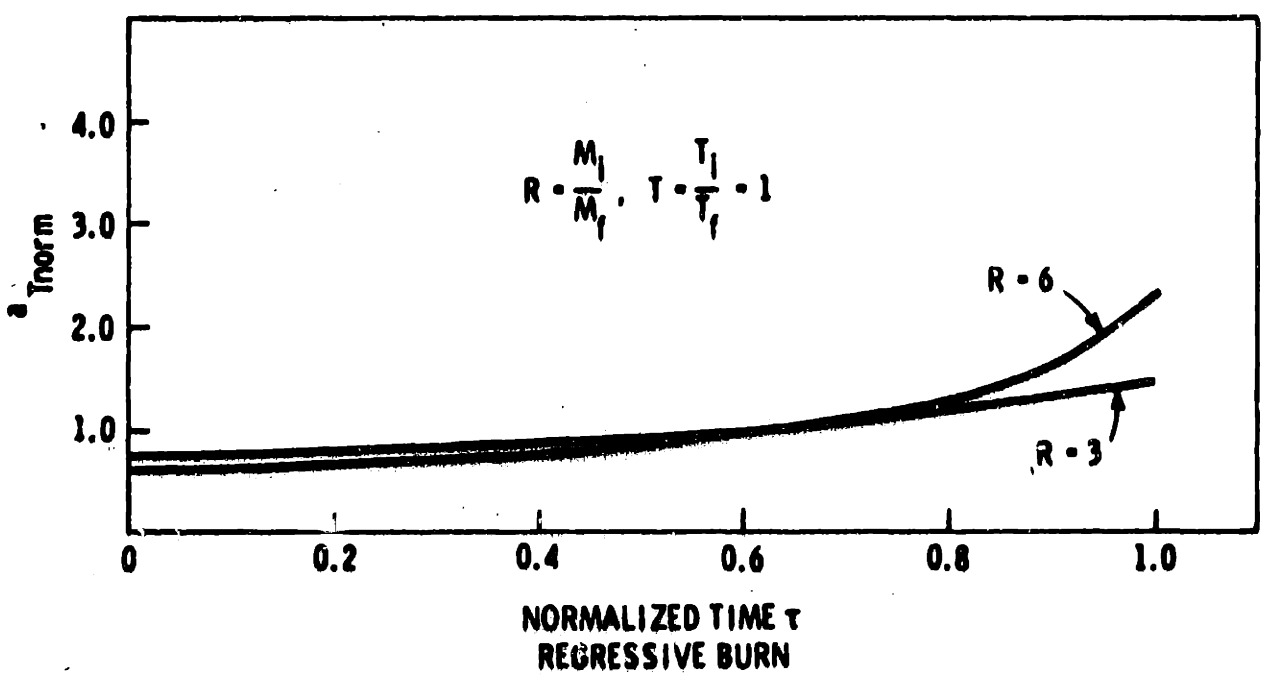

Fig. 3-8 Normalized a_t vs normalized time τ.

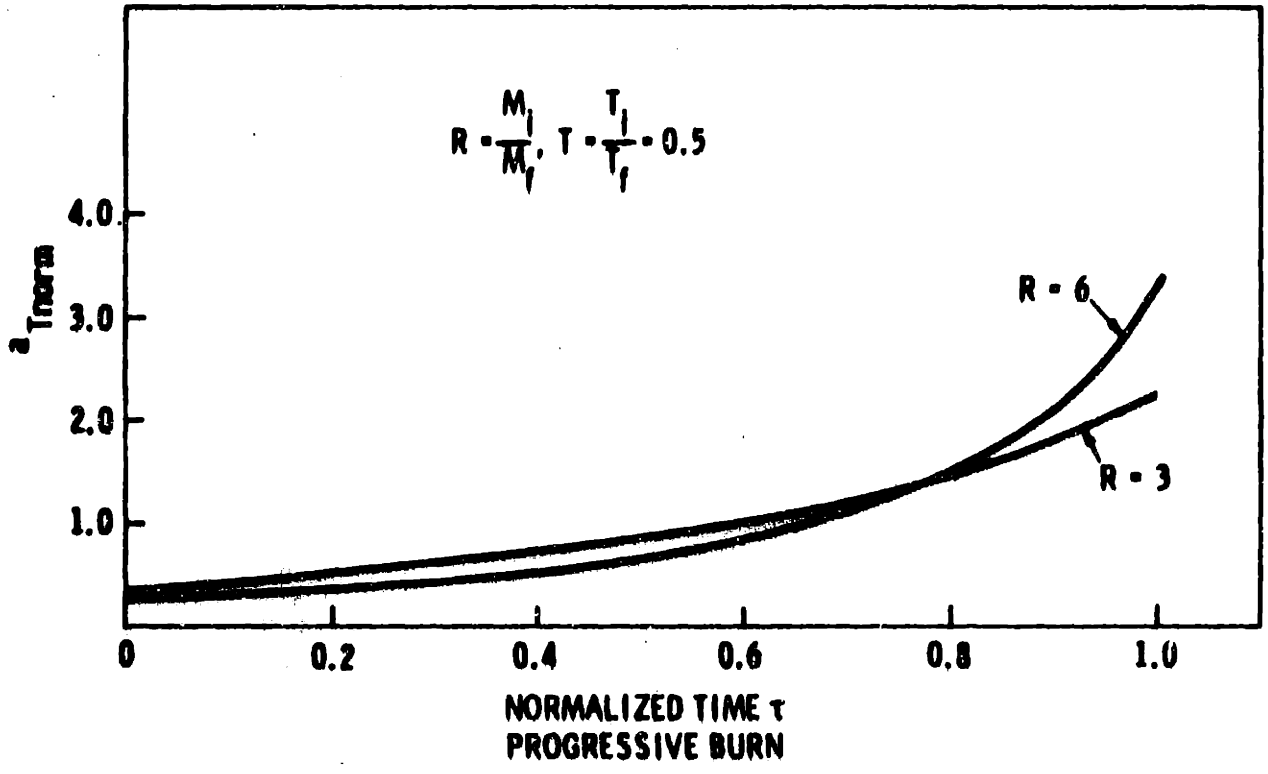

Fig. 3-9 Normalized a_t vs normalized time τ.

where

$$y' = dy/dx, \quad y'' = d^2y/d^2x \tag{3.25}$$

Using 3.24 Ω is found by

$$\Omega = \frac{a_T}{RADCURV} \text{ radians/sec} \tag{3.26}$$

Figures 3.7, 3.8 and 3.9 are plots of Ω_{norm} using R = 3, T = 1, and different values of ΔV_r.

Where Ω_{norm} is defined as

$$\Omega_{norm} = \Omega \, a_{Tnorm} \text{ radians/burn time} \tag{3.27}$$

The final angular velocity Ω_{fnorm}* has great importance and as pointed out by comparison of Figures 3.10, 3.11 and 3.12 Ω_{fnorm} increases with decreasing values of ΔV_r. Notice that the -45° position for initial $\underline{V}_g$ poses a problem. The curvature for the trajectories are severe and with the vertex located fairly near the terminal. As a result the angular acceleration is high traversing the nose of the parabola.

* $\Omega_f = \Omega_{fnorm}$

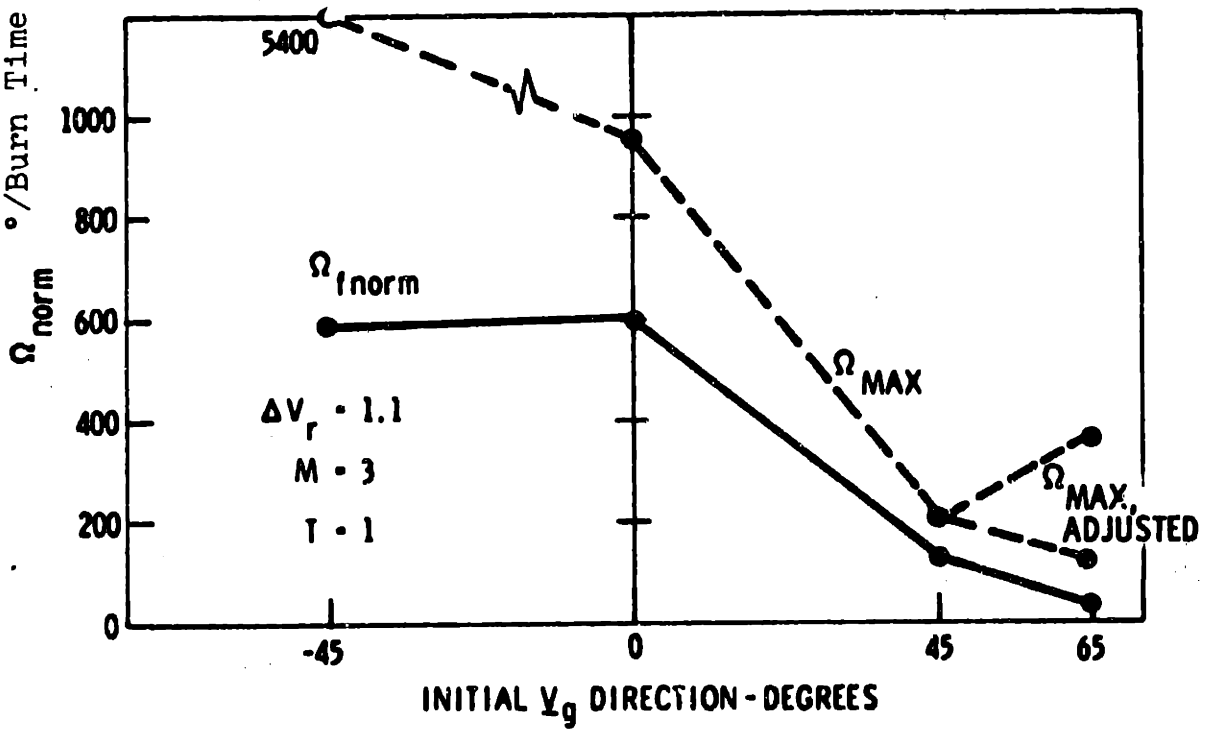

Fig. 3-10 Ω_{norm} parabola guidance ($\Delta V = 1.1$).

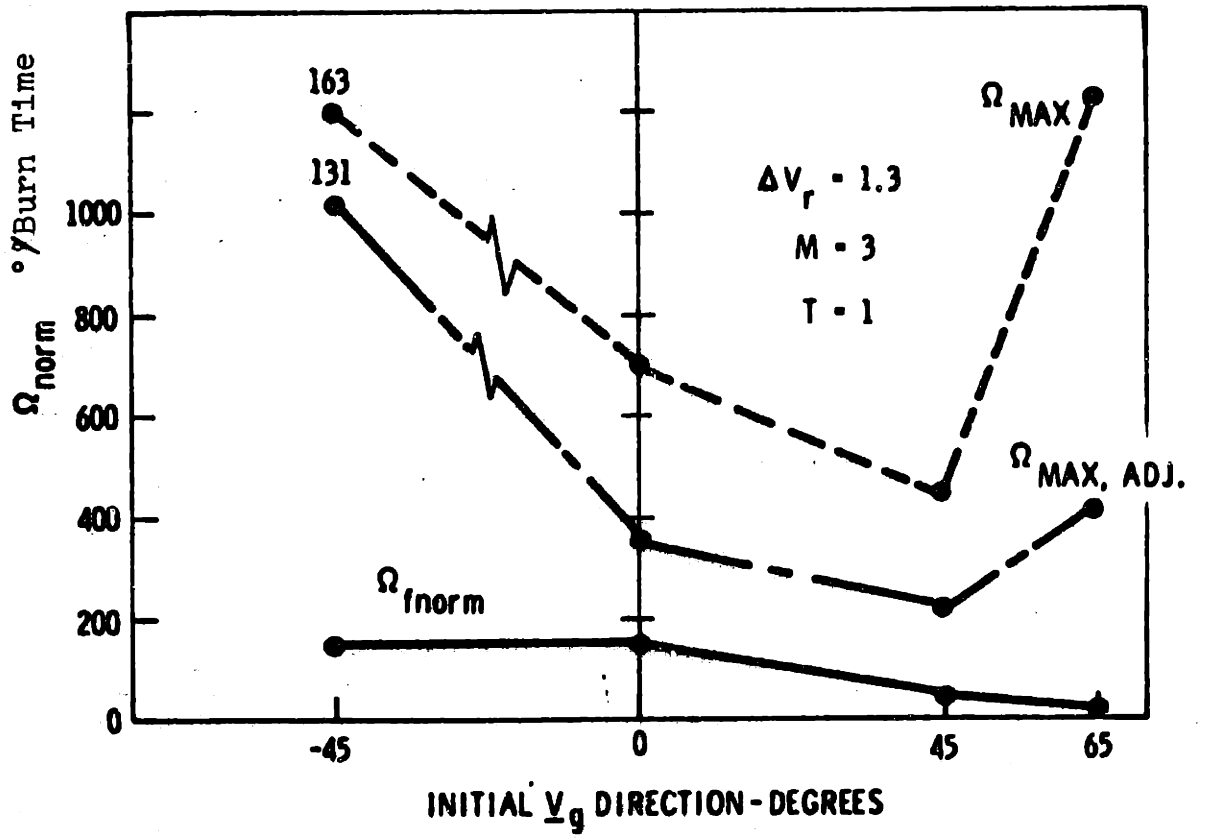

Fig. 3-11 Ω_{norm} parabola guidance ($\Delta V_r = 1.3$).

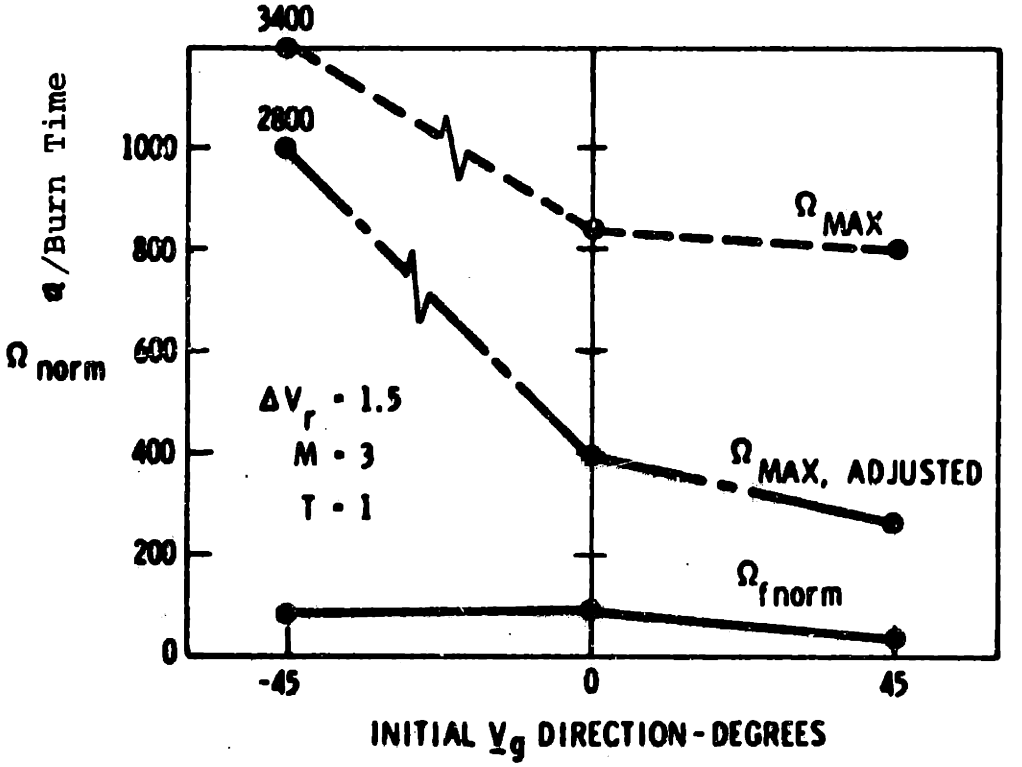

Fig. 3-12 Ω_{norm} parabola guidance ($\Delta V_r = 1.5$).

to the final position. Ω_f is the value of the angular velocity at $\underline{V}_g = (0, 0)$. The Ω_{max} curves represent a worst on worst case situation where the maximum thrust acceleration occurs at a point of minimum radius of curvature (which is the vertex of the parabola). When the vertex of the curve is far from the terminal point, then the acceleration must be adjusted to present realistic maximum angular velocities. The $\Omega_{max,adj}$ are nearly equal for the -45° initial $\underline{V}_g$ position. The Ω_f is quite low for ΔV_r equal to 1.3 and 1.5. Ω_f for ΔV_r equal to 1.1 is rather high until the initial $\underline{V}_g$ direction approaches 45°. It must be remembered that the curves are for particular values of R = 3 and T = 1.

As discussed in Section 3.1 perturbations effects will require periodic updating of the parabolic trajectory. Because of the time required for the update, the computation must be done at a rate slower than the thrust direction command $\underline{P}_c$ to the autopilot. The sequence may be that as shown in Figure 3.13.

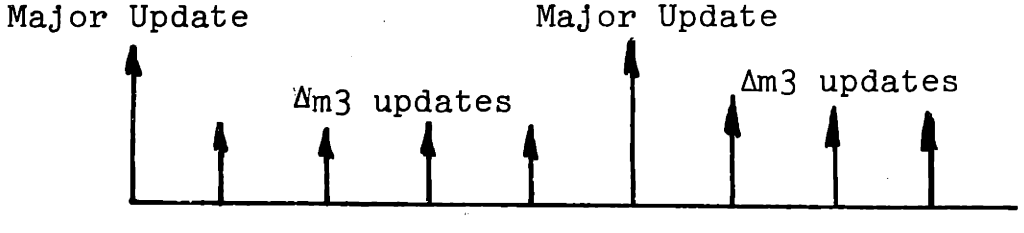

Parabola Update Rates

Figure 3.13

The slow rate time intervals compute the desired slope based on the present values of $\underline{V}_g$ and ΔV. The faster $\underline{P}_c$ command rates are based on an estimate of the slope change m3 during the time interval. m3 is estimated to first order by

$$\Delta m3 = \frac{(ARC1-ARC2)2}{(1 + m3^2)^{3/2} P} \tag{3.28}$$

where

ARC1 - last value of ΔV arc expended

ARC2 - present value of ΔV arc expended

P - parameter of parabola

Each high rate interval updates m3 by

$$m3 = m3 + \Delta m3 \tag{3.29}$$

$\Delta m3$ is invariant between coordinate systems and can be treated as a small rotation of $\underline{P}_c$.

The new $\underline{P}_c$ is calculated by

$$\underline{P}_c = \underline{P}_c + (\underline{P}_c \times \Delta \underline{m3}) \tag{3.30}$$

where

$$\underline{m3} = m3 \text{ UNIT } (\underline{I}.S.D. \times \underline{P}_c) \tag{3.31}$$

Summarizing the discussion of 3.2, the parabola proves to be a flexible contour with an arc length which is readily computed. The slope is conveniently updated at faster sampling rates between the major parabolic update times. The iteration

procedure converges rapidly with a good initial estimate. The parabola does in some cases impose a severe curvature on the trajectory, particularly as the initial $\underline{V}_g$ direction approaches -45°. The parabola cannot be curve fit if the initial $\underline{V}_g$ direction is $\pm$90° and the I.S.D. is $\pm$90°.

3.3 Circle-Line Guidance

Another explicit method computes a ΔV_r trajectory which is a combination of straight line and circular arc to provide the proper arc length of ΔV_r. It is interesting to note that this is the trajectory solution for the optimal minimum-time problem discussed in Chapter II. In the minimum-time solution the straight line was tangent to a circle of minimum radius which represented the maximum turning rate of the vehicle. In the applications being considered in this thesis (no terminal thrust control) the combined arc length must be controlled which implies the radius of the circle will vary to satisfy the arc length constraint.

Refer to Figure 3.14 for the following derivation.

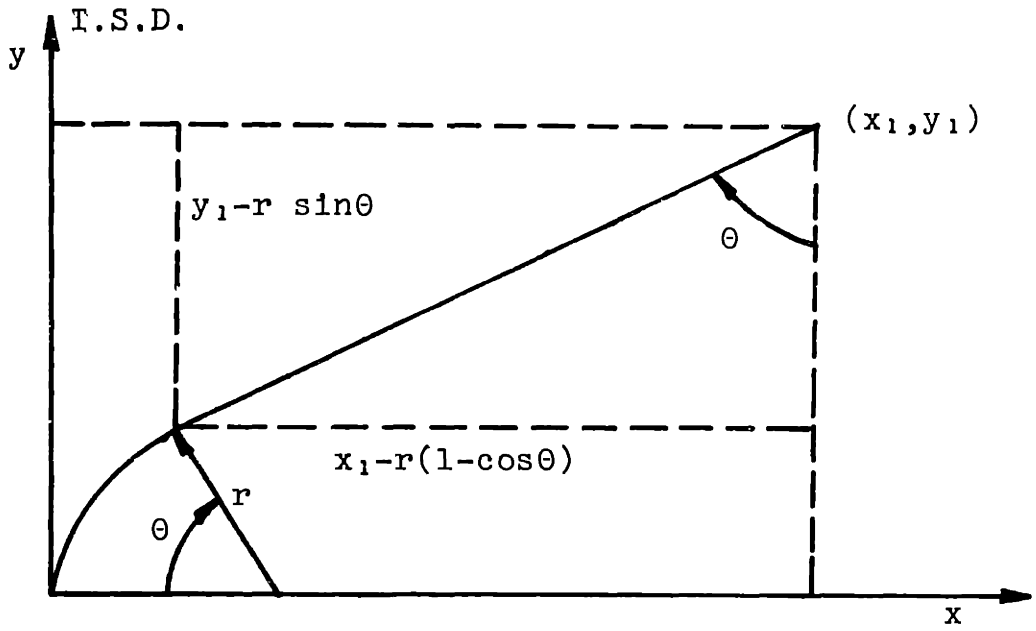

Line-Circle Guidance

Figure 3.14

Given: S, x_1, y_1

where S is the arc length and (x_1, y_1) is the initial $\underline{V}_g$ position

Find:

r, θ such that $r \geq r_{min}$ and the arc length S constraint is satisfied

From Figure 3.14

$$S = r\,\theta + (x_1 - r\,(1-\cos\theta))/\sin\theta \qquad (3.32)$$

$$\cos\theta = (y_1 - r\sin\theta)/(x_1 - r(1-\cos\theta)) \tag{3.33}$$

Solve 3.27 for r

$$r = (x_1\cos\theta - y_1\sin\theta)/(\cos\theta - 1) \tag{3.34}$$

The derivative of S with respect to θ is

$$\frac{ds}{d\theta} = \frac{dr}{d\theta}\left(\theta - \frac{(1-\cos\theta)}{\sin\theta}\right) + \frac{r(1-\cos\theta)\cos\theta}{\sin^2\theta} \tag{3.35}$$

$$- \frac{x_1\cos\theta}{\sin^2\theta}$$

where

$$\frac{dr}{d\theta} = (y_1(\cos\theta - 1) + x_1\sin\theta)/(\cos\theta-1)^2 \tag{3.36}$$

The procedure to calculate r and θ is the following:

1. Guess θ, given x_1, y_1, and S.

2. Calculate

   r from 3.28

   S_1 from 3.26

3. Compute δθ by

$$\delta\theta = (S-S_1)/(ds/d\theta) \tag{3.37}$$

4. Repeat with $\theta = \theta + \delta\theta$ until $S-S_1$ is less than a specified tolerance.

Then the desired direction of the thrust acceleration is along the straight line defined by θ until $|\underline{V}_g|$ is less than $r\dot{\theta}$. When $|\underline{V}_g| < r\dot{\theta}$, the direction is defined by the tangent to the circular arc.

The ΔV_r trajectories for the line-circle combination were analyzed in the same manner as was done in Section 3.2 for the parabola. The data for ΔV_r = 1.1, 1.3 and 1.5 is presented in Figures 3.15, 3.16 and 3.17. Again the insensitive direction is chosen arbitrarily along the positive vertical axis. As the initial $\underline{V}_g$ direction swings toward the I.S.D., the limit of the problem solution is approached. Notice in Figure 3.17 that 0° is very near the solution of being on the circular arc the entire trajectory. As the $\underline{V}_g$ direction rotates toward -90°, there is great flexibility with an attendant penalty in arc curvature. If there is no circle-line solution for a $\underline{V}_g$ direction, the I.S.D. may be chosen 180° from the present one. The solutions would then be a mirror image of the curves shown in 3.15, 3.16 and 3.17. Notice that $\pm$90° solution are possible.

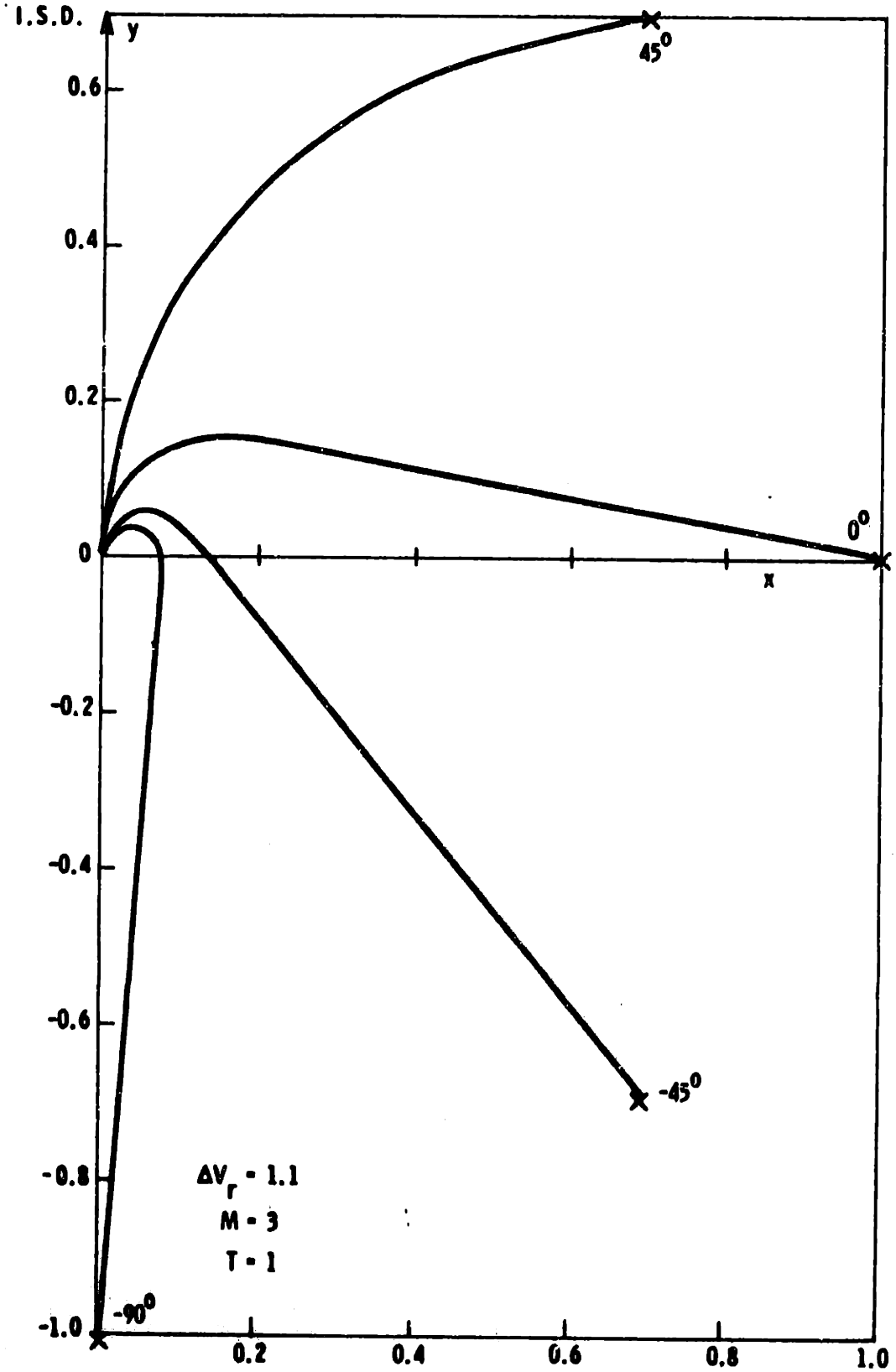

Fig. 3-15 Line-circle trajectories ($\Delta V_r = 1.1$).

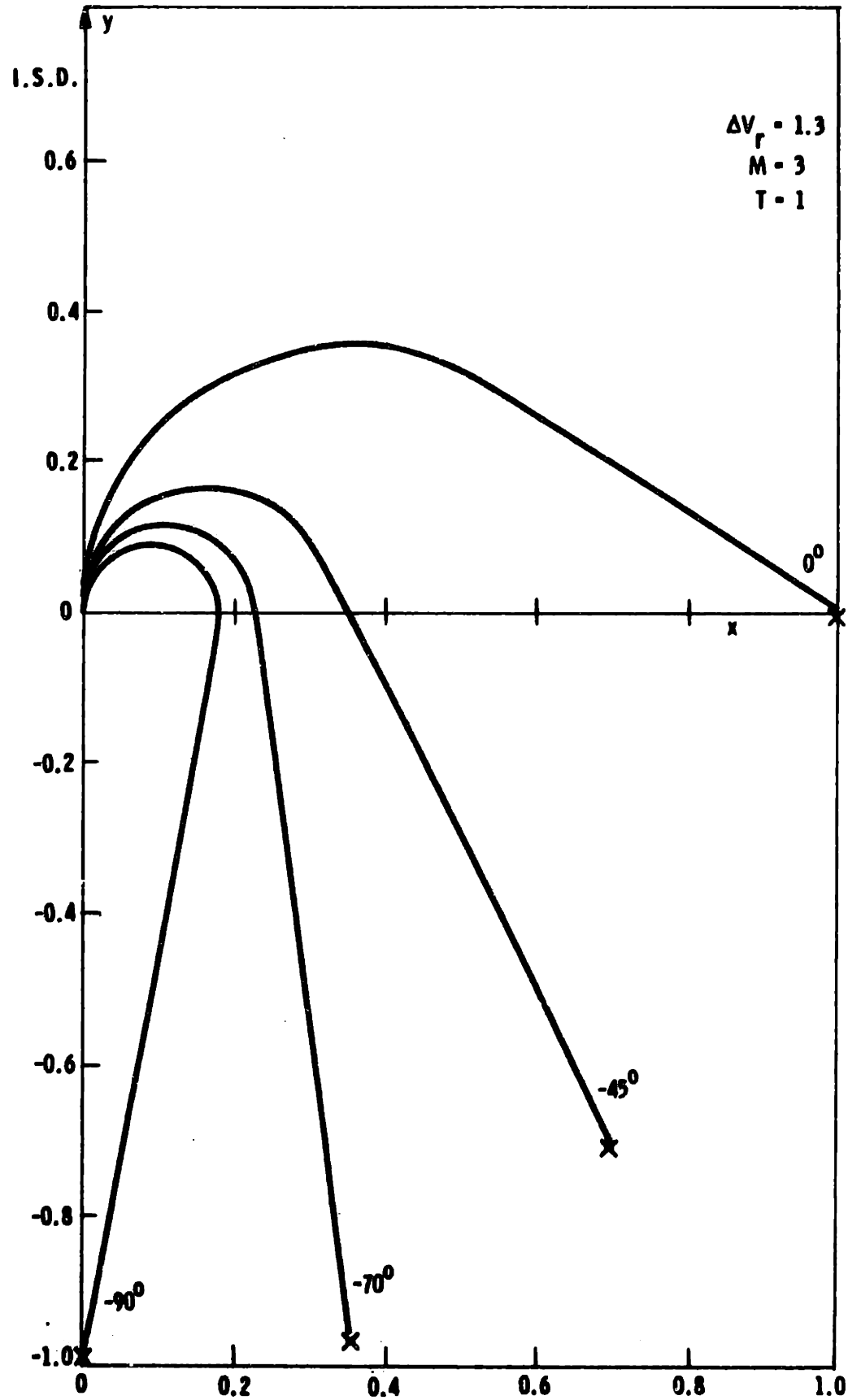

Fig. 3-16 Line-circle trajectories ($\Delta V_r = 1.3$).

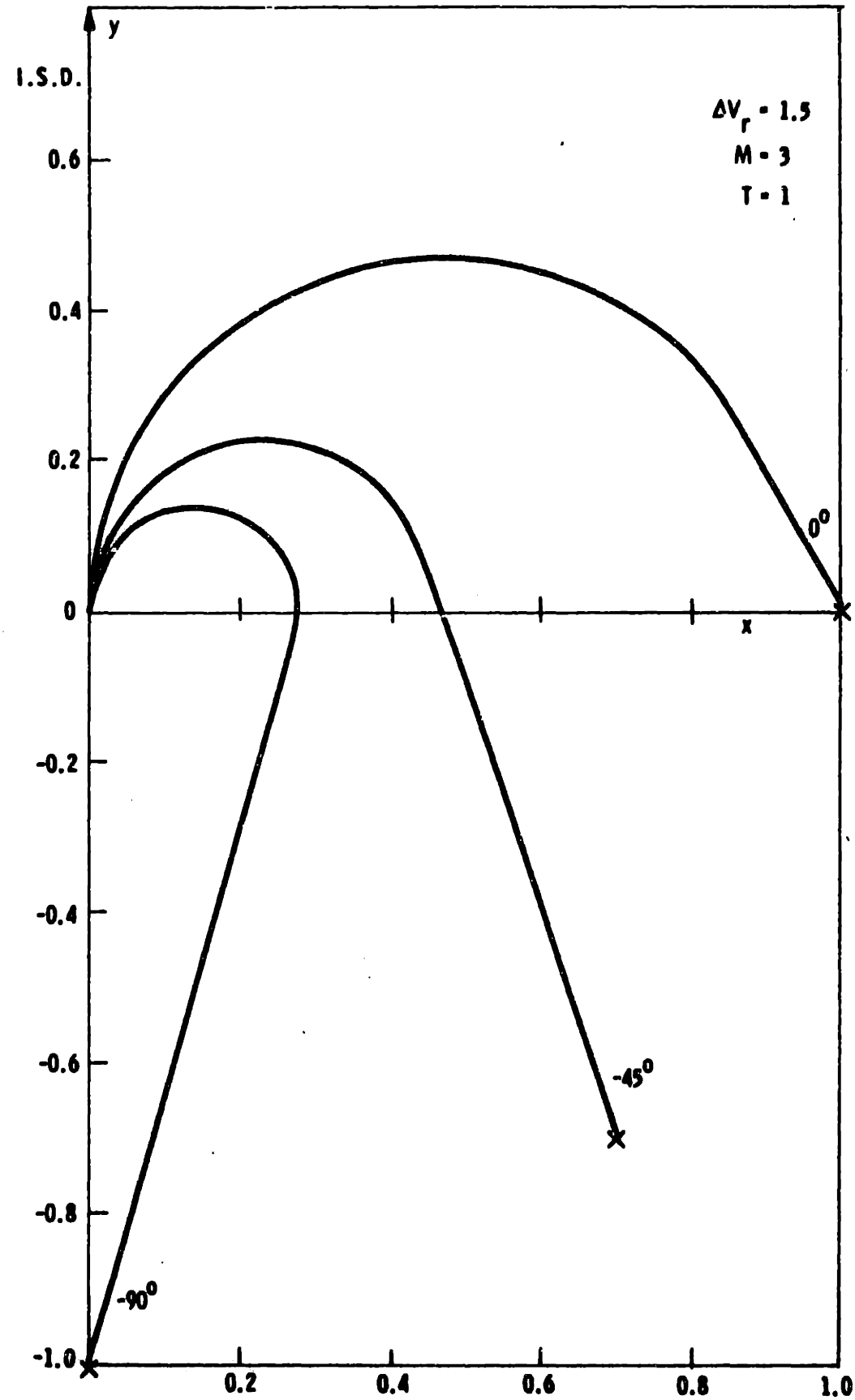

Fig. 3-17 Line-circle trajectories ($\Delta V_r = 1.5$).

The normalized angular velocities are shown in Figure 3.18. For the line-circle, Ω_f and Ω_{max} are the same. The angular velocity commanded from the line into the circle is a step input.

Comparisons of the parabola and the line-circle methods results in the following:

1. The line-circle requires considerably less computation.
2. The parabola is generally more flexible in terms of being fit from a $\underline{V}_g$ direction.
3. An exception to 2 is the $\pm 90°$ direction which the line-circle can handle but the parabola cannot.
4. The parabola exhibits less terminal angular velocity.
5. The maximum angular velocities required are essentially the same for $\Delta V_r = 1.1$. At larger ΔV_r, the line-circle has lower maximum rates as the $\underline{V}_g$ direction $\rightarrow -45°$.

The line-circle slope could be updated periodically as in the parabola method to account for perturbations. In the line-circle case the radius of curvature is r when on the circular arc. The slope is then updated by

$$\delta_{slp} = \delta_{arc}/r \tag{3.38}$$

$$slp = slp + \delta_{slp} \tag{3.39}$$

where

δ_{arc} is the expended ΔV over the update interval

δ_{SLP} is the change in slope

SLP is the value of the tangent to the circle of radius r at present ΔV_r position

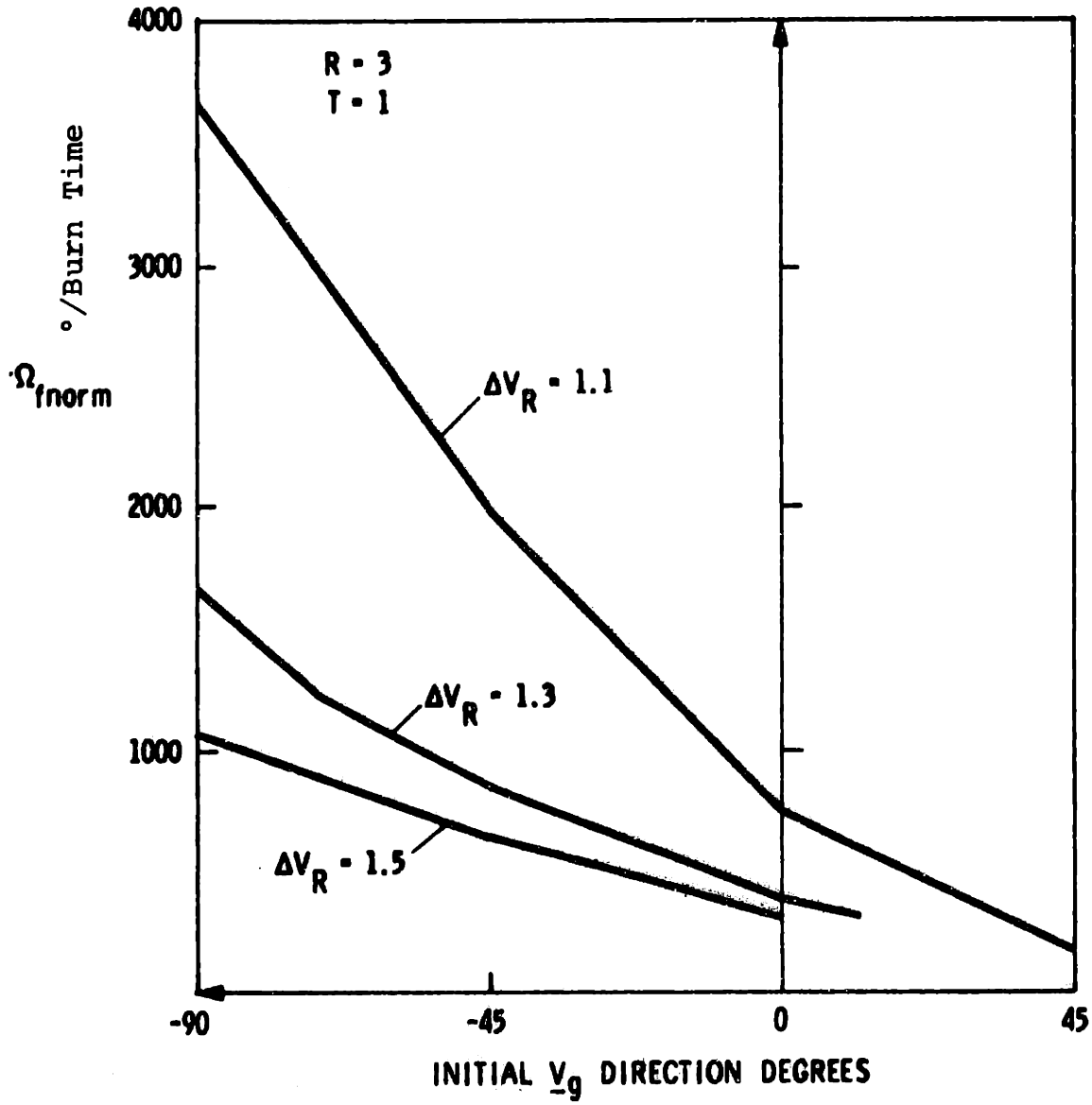

Fig. 3-18 Ω_{fnorm} for line-circle guidance.

CHAPTER IV

INSENSITIVE DIRECTION COMPUTATION

4.1 Null Range Direction

The null range direction is defined as the direction of thrusting on a body in an inverse square central force field such that the trajectory of the body is not displaced from a preselected inertial destination point. Thrusting in the null range direction changes the characteristics of the orbit, the time of flight (t_{ff}), and the velocity vector at the destination point. The null range direction varies in flight so that null range thrusting requires continuous alignment.

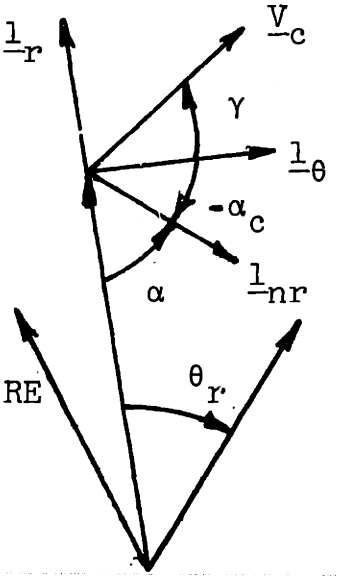

$\underline{R}$ = present position
$\underline{R}_T$ = target position
$\underline{l}_r$ = unit($\underline{R}$)
$\underline{l}_\theta$ = unit($\underline{R}\times\underline{R}_T\times\underline{R}$)
θ_r = range to go
γ = flight path angle
$\underline{V}_c$ = correlated velocity
α = null range angle
RE = earth radius
$\underline{l}_{nr}$ = null range direction

Null Range Direction Definition

Figure 4.1

There are a number of ways of defining the null range direction. In this thesis the null range angle α will be defined from the $-\underline{l}_r$ direction as shown in Figure 4.1. $\underline{l}_{nr}$ is the null range direction.

Define

$$V_{cr} = |\underline{V}_c| \sin\gamma$$
$$V_c = |\underline{V}_c| \cos\gamma \tag{4.1}$$

Wheelon[4] derives the 'hit' equation which may be put in the form

$$V_{cr} = \frac{E\, R_t\, (1-\cos\theta_r) - R_m\, V_{c\theta}^2 (R_m - R_t \cos\theta_r)}{R_m\, R_t\, V_{c\theta} \sin\theta_r} \tag{4.2}$$

where

E is the gravitational product of the earth

$R_m = |\underline{R}|$

$R_t = |R_t|$

θ_r is the range angle to go

Therefore, V_{cr} is the function

$$V_{cr} = V_{cr}\,(R_t, R_m, V_{c\theta}) \tag{4.3}$$

Holding R_t and R_m constant and taking the partial of 4.3 with respect to V_c gives

$$\frac{\partial V_{cr}}{\partial V_{c\theta}} = \frac{-(R_m - R_t \cos\theta_r)}{R_t \sin\theta_r} - \frac{E(1-\cos\theta_r)}{R_m V_{c\theta}^2 \sin\theta_r} \qquad (4.4)$$

From 4.2

$$\frac{-E(1-\cos\theta_r)}{R_m V_{c\theta}^2 \sin\theta_r} = \frac{-V_{cr}}{V_{c\theta}} - \frac{(R_m - R_t \cos\theta_r)}{R_t \sin\theta_r} \qquad (4.5)$$

Using 4.5 in 4.4

$$\frac{\partial V_{cr}}{\partial V_{c\theta}} = \frac{-V_{cr}}{V_{c\theta}} - 2\,\frac{(R_m - R_t \cos\theta)}{R_t \sin\theta_r} \qquad (4.6)$$

Using the geometry of Figure 4.2

$$\frac{\partial V_{cr}}{\partial V_{c\theta}} = -\tan\gamma - 2\cot\phi \qquad (4.7)$$

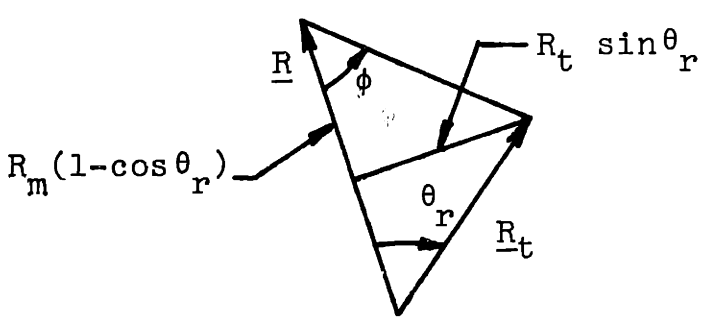

Figure 4.2

Definition of ϕ

Therefore

$$\alpha_c = \tan^{-1} \frac{\partial V_{cr}}{\partial V_{c\theta}} \tag{4.8}$$

defines a direction along which an incremental velocity change may occur and still allow the body to intersect the desired inertial destination point. Since we are defining α from the $-\underline{l}_r$ direction

$$\alpha = \frac{\pi}{2} + \alpha_c \tag{4.9}$$

Notice in Equation 4.4 through 4.9 that t_{ff} is free to vary so that velocity changes in the α direction change the time of free-fall.

Graphs of the null range angle α versus the range-to-go θ_R are shown in Figures 4.3, 4.4, and 4.5. At shorter ranges (under 10°) α is a more volatile function of altitude and range. At longer ranges, α is well behaved and nearly linear with altitude.

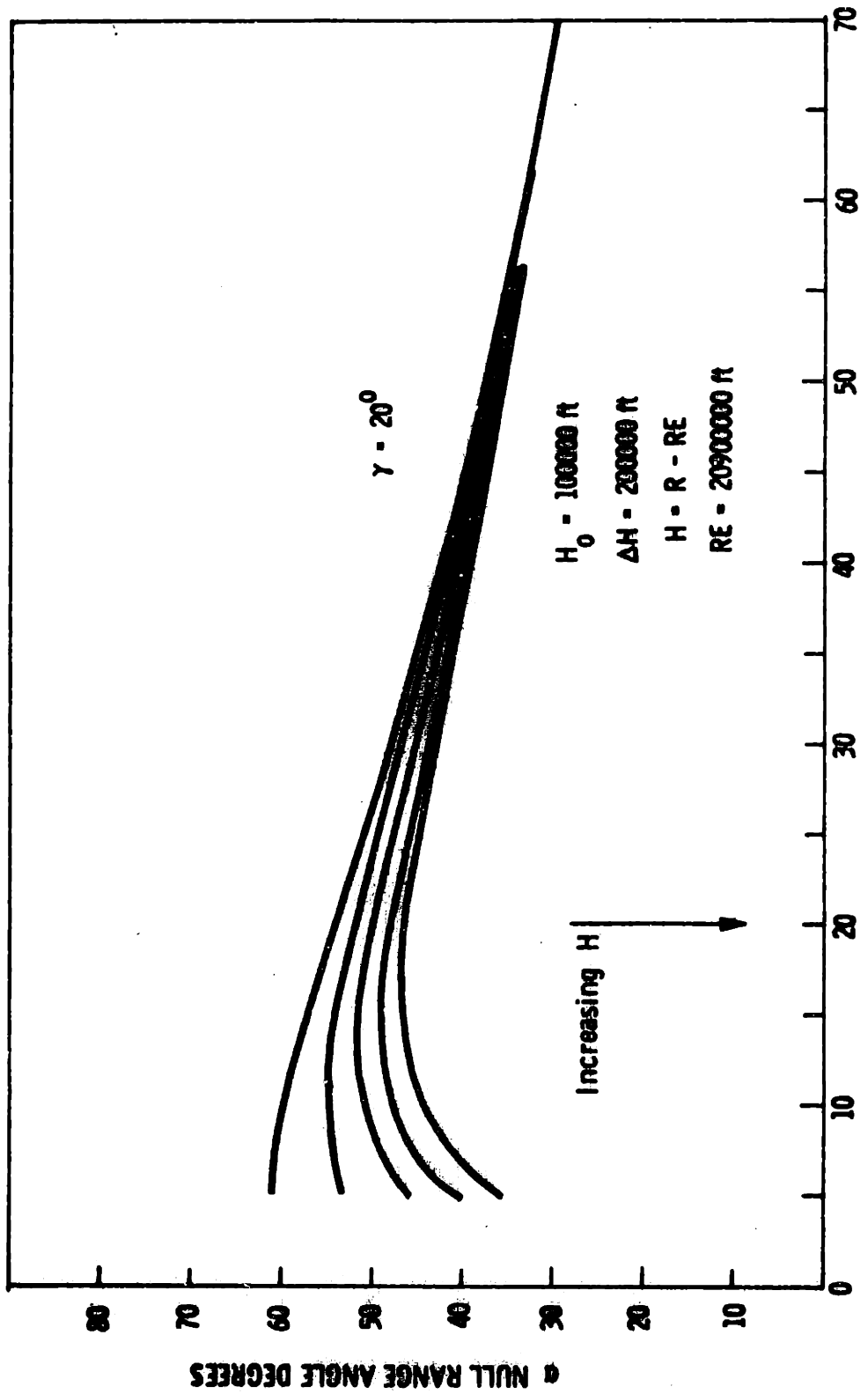

Fig. 4-3 Null range angle vs θ_r ($\gamma = 20^o$).

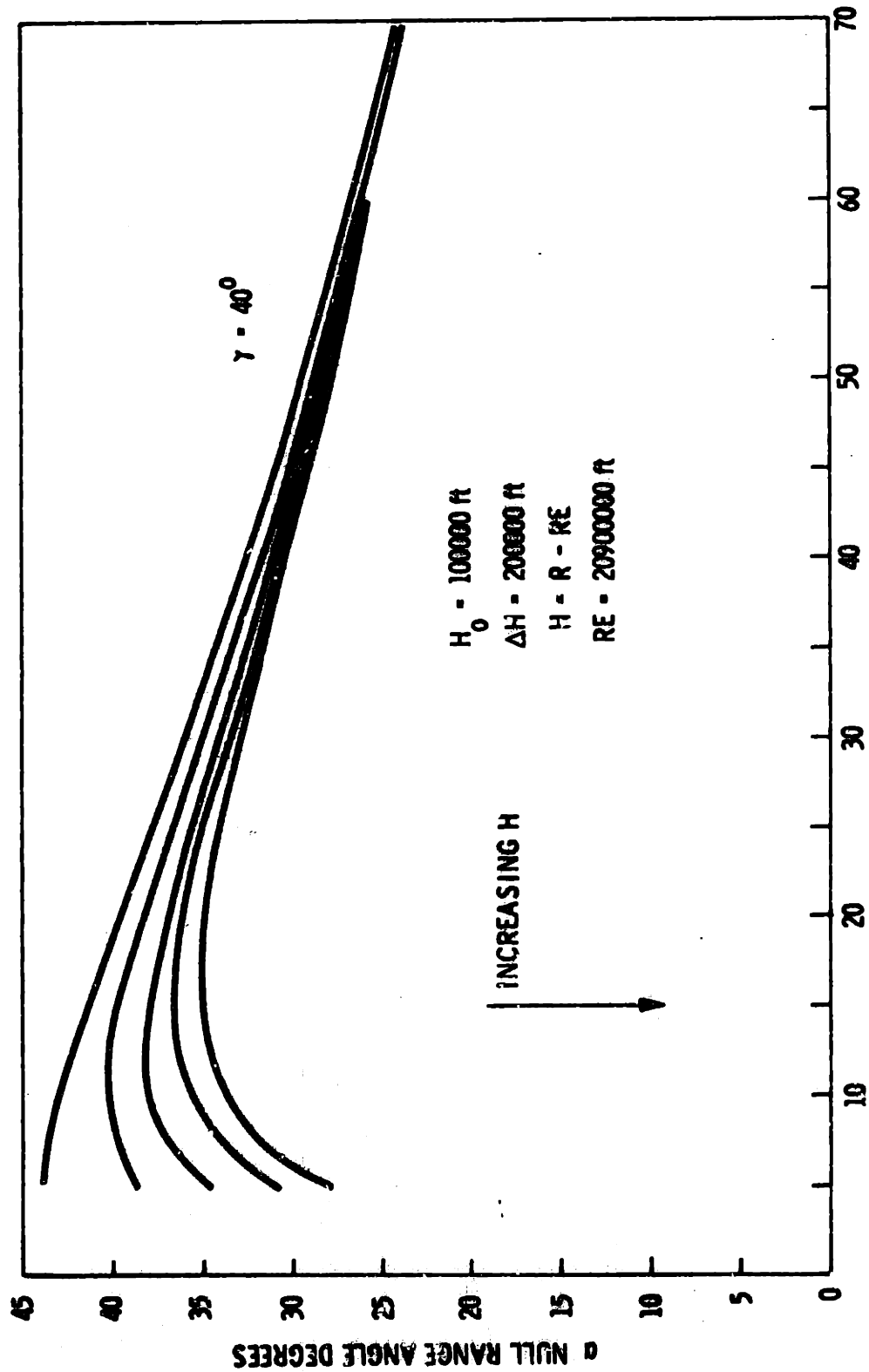

Fig. 4-4 Null range angle vs θ_r ($\gamma = 40^0$).

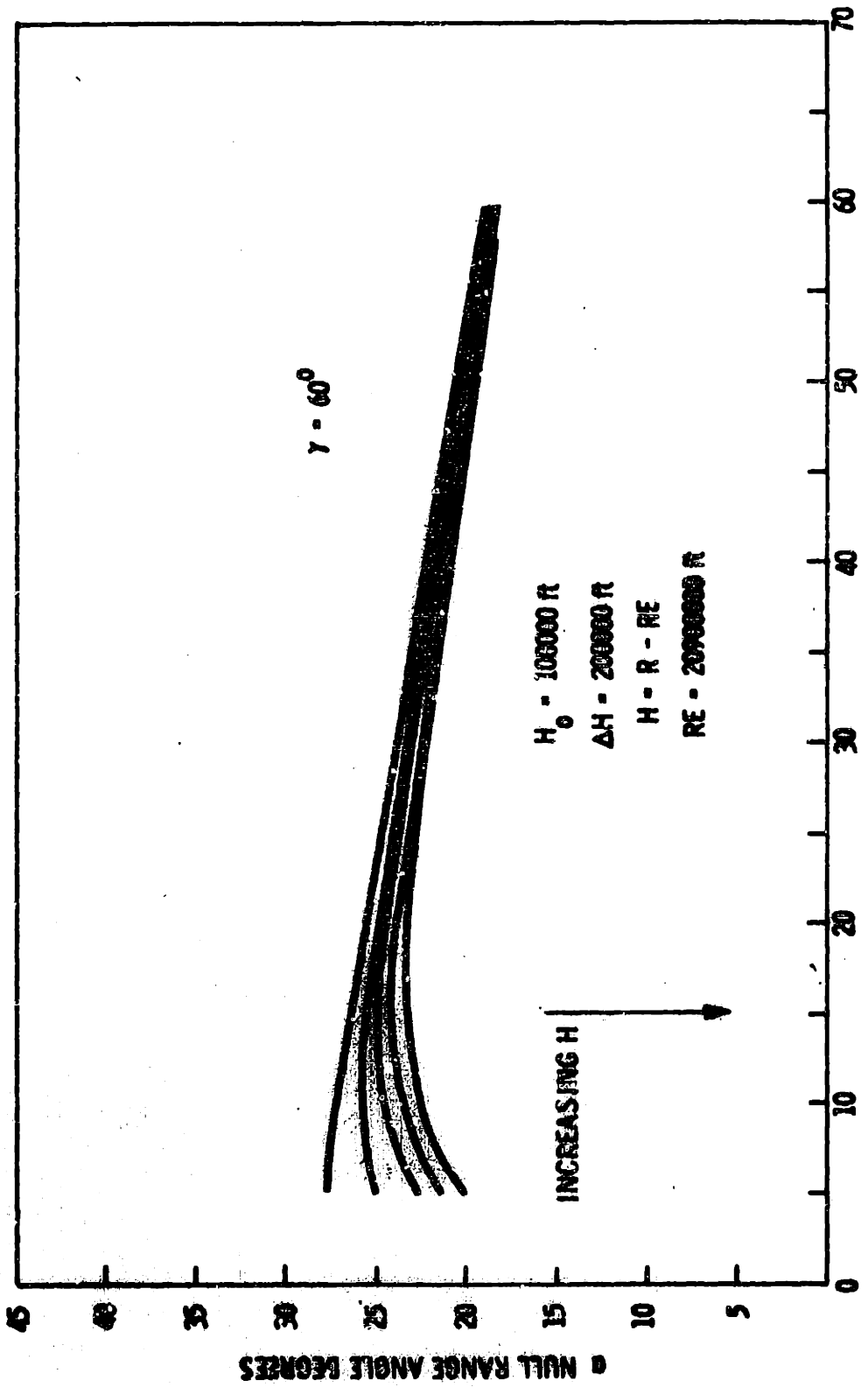

Fig. 4-5 Null range angle vs θ_r ($\gamma = 60^o$).

CHAPTER V

RESULTS

5.1 Introduction

A digital simulation of the parabolic guidance law was developed to pursue further analysis. Basic objectives of the analyses were to establish broad autopilot requirements and to determine suitable intervals for the major parabolic update and the faster intermediate slope computation. The parabola trajectory was tested for various conditions of initial $\underline{V}_g$ direction, ΔV_r ratios, and thrust force profiles. In addition, the effect of the $Q\underline{V}_g$ contribution was tested. A run demonstrating the sensitivity to an initial offset between $\underline{P}$ and $\underline{P}_c$ was performed.

The problem of terminal settling dynamics into the I.S.D. is not covered in this thesis, and is an area of further investigation. The vehicle terminal angular velocity has to be reduced to zero, and the $\underline{V}_g$ nulled along the I.S.D. One possible approach is to estimate the effect of the terminal dynamics on $\underline{V}_g$ and to allow for this in the guidance calculation. Another approach might use a curve fit which exhibits zero curvature at the terminal point. This would impose computational difficulties on the arc length computation.

A third scheme could be implemented which nulls the $\underline{V}_g$ along the I.S.D. near the time of fuel depletion. This would require switching between control laws at the proper time.

The line circle guidance law was partially checked under simulation conditions. The basic problem encountered was a suitable guidance scheme to handle perturbations during the circular arc segment. This also is an area of further development.

An illustration of the performance of the optimal specified time problem which was discussed in Chapter II is presented in Section 5.4.

5.2 Autopilot Requirements

The steering control which was discussed in Section 1.1 was used in the simulation. A block diagram is shown in Figure 5.1.

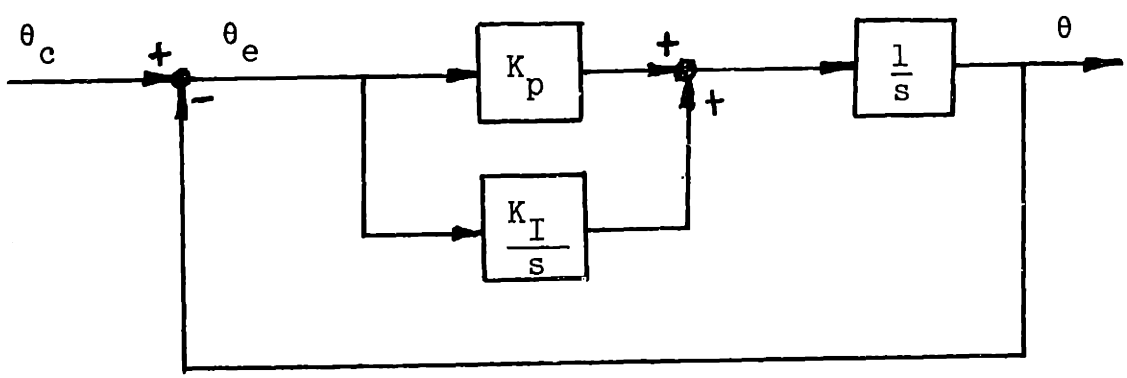

Figure 5.1

where θ_c is the angle of $\underline{P}_c$ referenced to the x axis

θ_p is the angle of $\underline{P}$ = Unit($\underline{a}_T$) referenced to the x axis

The closed-loop performance function is

$$PF_{cl} = \frac{K_I + K_p s}{s^2 + K_p s + K_I} \tag{5.1}$$

The Laplace transform of θ_e is

$$\theta_e(s) = \frac{\theta_c(s)\, s^2}{s^2 + K_p s + K} \tag{5.2}$$

If $\theta_c(s) = \frac{\theta_c}{s^2}$, the following error is

$$\theta_e(\infty) = \lim_{s \to 0} \frac{s\theta_c}{s^2 + K_p s + K_I} = 0 \tag{5.3}$$

Therefore the control law follows a ramp $\theta_c(t)$ input with zero error. Values of $K_p = 21 \frac{rad}{sec}$, and $K_I = 225 \frac{rad^2}{sec^2}$ were found to perform satisfactorily under the simulation conditions. These values correspond to a bandwidth or break

frequency of 10 rad/sec and a damping ratio of .7. When the bandwidth was lowered to 5 rad/sec, the autopilot response was not fast enough for the cases involving a small radius of curvature and the simulation failed. The initial $\underline{V}_g$ direction of -45° is an example. In such cases the negative insensitive direction can be used.

A high value of Ω_f is undesirable in terms of autopilot requirements. As discussed in Section 5.1, the vehicle must settle into the I.S.D. while nulling the $\underline{V}_g$.

5.3 Parabolic Guidance Simulation Results

The parabolic guidance law was tested in the digital simulation using ΔV_r ratios of 1.1, 1.3 and 1.5. For these three ratios initial $\underline{V}_g$ directions of -45°, 0°, and 45° were chosen. During these runs, the parabolic update was performed at the fast update period of .01 seconds. The terminal conditions at fuel depletion are presented in Table 5.1. As discussed in Section 5.2, values of K_p = 21 rad/sec and K_I = 225 rad^2/sec^2 were used along with a mass ratio of R = 3 and a thrust force profile T = 1. A rate limit of 2 rad/sec was imposed on the autopilot. The simulations made from the -45° initial $\underline{V}_g$ direction failed because of the rate limiting. The failure occurred in the parabola guidance which could not successfully converge on a parabola which exhibited extremely sharp curvature. The remaining runs proved successful as demonstrated by Table 5.1. The very small number for the terminal conditions reflect the fact that there is no computer word length quantization in the simulation.

Note the Ω_{fnorm} values are not zero in Table 5.1. This points out the fact that the figures in the table do not include the effect of settling into a fixed thrusting orientation along the insensitive direction. As discussed previously, this problem is not solved in the thesis.

Table 5.1 also demonstrates the penalty of a larger Ω_{fnorm} as the ΔV_r becomes smaller. For the 0° case, Ω_{fnorm} for $\Delta V_r = 1.3$ is less than one-third of that for $\Delta V_r = 1.1$. Another observation, which was discussed in Chapter III, is that as the initial $\underline{V}_g$ direction swings toward the I.S.D., Ω_{fnorm} is reduced dramatically. Note for $\Delta V_r = 1.1$, the Ω_{fnorm} of 45° is 25% that of the 0° case.

Graphs of some typical runs from Table 5.1 are shown in Figures 5.2 through 5.7. In Figure 5.3 when $\Delta V_r = 1.1$, the parabola vertex is quite close to the terminal and consequently Ω_{fnorm} is quite high. As ΔV_r is increased (Figure 5.5), the $\Omega_{norm}(t)$ profile is much less severe and the maximum angular velocity requirements are spread further from the terminal point. The measure of unit($\underline{a}_T$) misalignment at fuel depletion in Figure 5.2, 5.4, 5.6 is P_x. The P_x profiles reflect the angular velocity histories mentioned above. As ΔV_r increases the slope of P_x is less steep near the terminal.

TABLE 5.1 PARABOLIC SIMULATION RESULTS (1)*

ΔV_r	$\underline{V}_g(0)$ DIR.°	$V_{gx}(t_b)$	$V_{gz}(t_b)$	$P_x(t_b)$ mrad	fnorm RAD/B.T.	REMARKS
1.1	-45°					FAILED
1.1	0°	3.5 E-7	3.5 E-4	1.5	- 8.7	
1.1	45°	-2.6 E-8	8.6 E-4	.5	- 1.9	
1.3	-45°					FAILED
1.3	0°	-5.8 E-8	5.2 E-4	.2	- 2.4	
1.3	45°	-3.6 E-8	7.8 E-4	9 E-2	- .7	
1.5	-45°					FAILED
1.5	0°	-3 E-8	4 E-4	.3	- 1	
1.5	45°	-3.5 E-8	5.1 E-4	-1.3 E-2	- .47	

* E symbolizes exponent to base 10

TABLE 5.2 PARABOLIC SIMULATION RESULTS (2)

ΔV_r	$\underline{V}_g(0)$ DIR.	$V_{gx}(t_b)$	$V_{gz}(t_b)$	$P_x(t_b)$ mrad	fnorm RAD/B.T.	REMARKS
1.1	0°	1.1 E-6	4.2 E-4	2.3	- 11.6	QV_g
1.1	0°	1.2 E-8	2.9 E-4	1	- 7.6	T=1.5
1.1	0°	1.0 E-6	5 E-4	2.7	- 11.2	T= .5
1.1	0°	9.2 E-6	5 E-4	.3	- 1	TPARAB= .25 sec
1.1	0°	1.8 E-7	3.7 E-6	- .3	- .9	30° OFFSET

The variable ETH is the misalignment between the commanded vector $\underline{P}_c$ and the thrust acceleration vector unit($\underline{a}_T$). The maximum value of ETH encountered in the runs of Table 5.1 was was less than 10 mrad.

Conditions for a standard run were selected as $\Delta V_r = 1.1$ and initial $\underline{V}_g$ direction = 0°. K_p and K_I values were kept the same. A run which introduced the $Q\underline{V}_g$ perturbation was performed using $Q_{xx} = Q_{zz} = -.001 \frac{1}{sec}$, and all other matrix elements zero. The terminal conditions are given in Table 5.2. The perturbation contribution slowly changed the coefficients of the parabola. Note, however, the 30% increase in the terminal Ω_{fnorm}. The effect of $Q\underline{V}_g$ on Ω_{fnorm} is significant at the lower values of ΔV_r. Since the direction of the I.S.D. is arbitrary, the effect of $Q\underline{V}_g$ will vary with the changing I.S.D. direction.

Progressive and regressive thrust force profiles were tested and the terminal fuel depletion conditions are given in Table 5.2. The only significant difference from the standard run (T = 1) was the value of Ω_{fnorm}. The progressive burn resulted in a 30% increase in Ω_{fnorm} while the regressive burn decreased Ω_{fnorm} by 10%.

A fast sampling period of .01 sec was found to be satisfactory. Successful runs were made using a parabola update period of .25 sec. The slope between major updates was computed as described in Chapter III. Fuel depletion

conditions for the standard simulation conditions are shown in Table 5.2. There is a 10% increase in Ω_{fnorm} caused by differences in autopilot behavior and the approximation made in the slope update.

The effect of an initial offset between unit($\underline{a}_T$) and $\underline{P}_c$ was tested using the standard run. An offset of 30° was used. The simulation ran successfully as verified by the results in Table 5.2 and the graph in Figures 5.7 and 5.8. ETH in Figure 5.8 has a large overshoot because the damping ratio is set at .7. ETH settles in a time constant

$$t_c = \frac{4}{\delta w_d} = \frac{4}{7} \text{ sec}$$

There is about a 5% increase in Ω_{fnorm} (when compared to a zero initial offset) caused by the ΔV expended during the initial settling period.

Summarizing the results of the simulation analysis of the parabola guidance

1. The -45° cases resulted in failure due to the rate limiting. This problem can be overcome by using the -I.S.D. direction.
2. Generally the simulation results are satisfactory for 0° and 45°. Zero degrees is not the limiting case. Runs approaching -45° which would not exceed the rate limit could have been made.

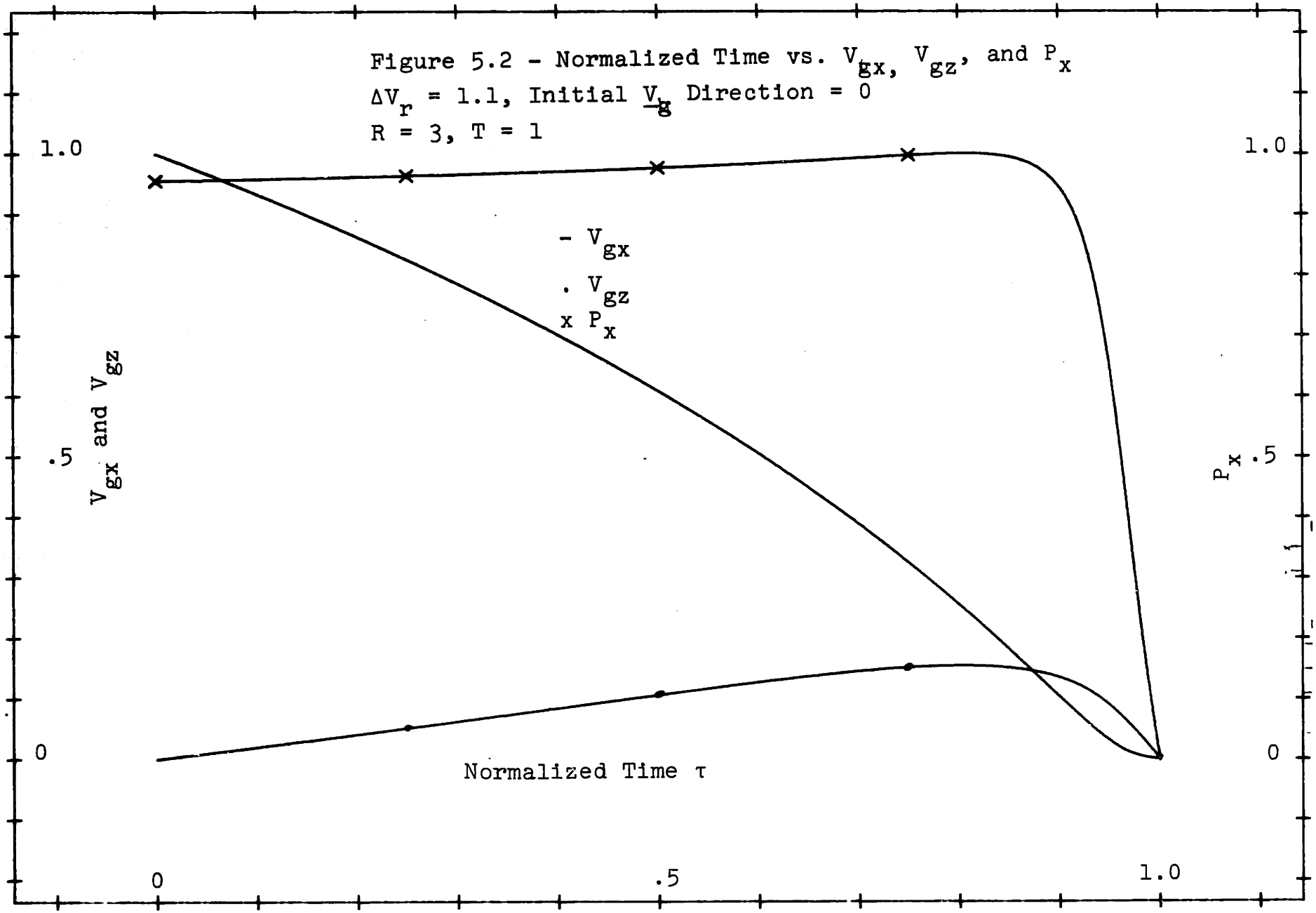

Figure 5.2 - Normalized Time vs. V_{gx}, V_{gz}, and P_x
ΔV_r = 1.1, Initial $\underline{V}_g$ Direction = 0
R = 3, T = 1

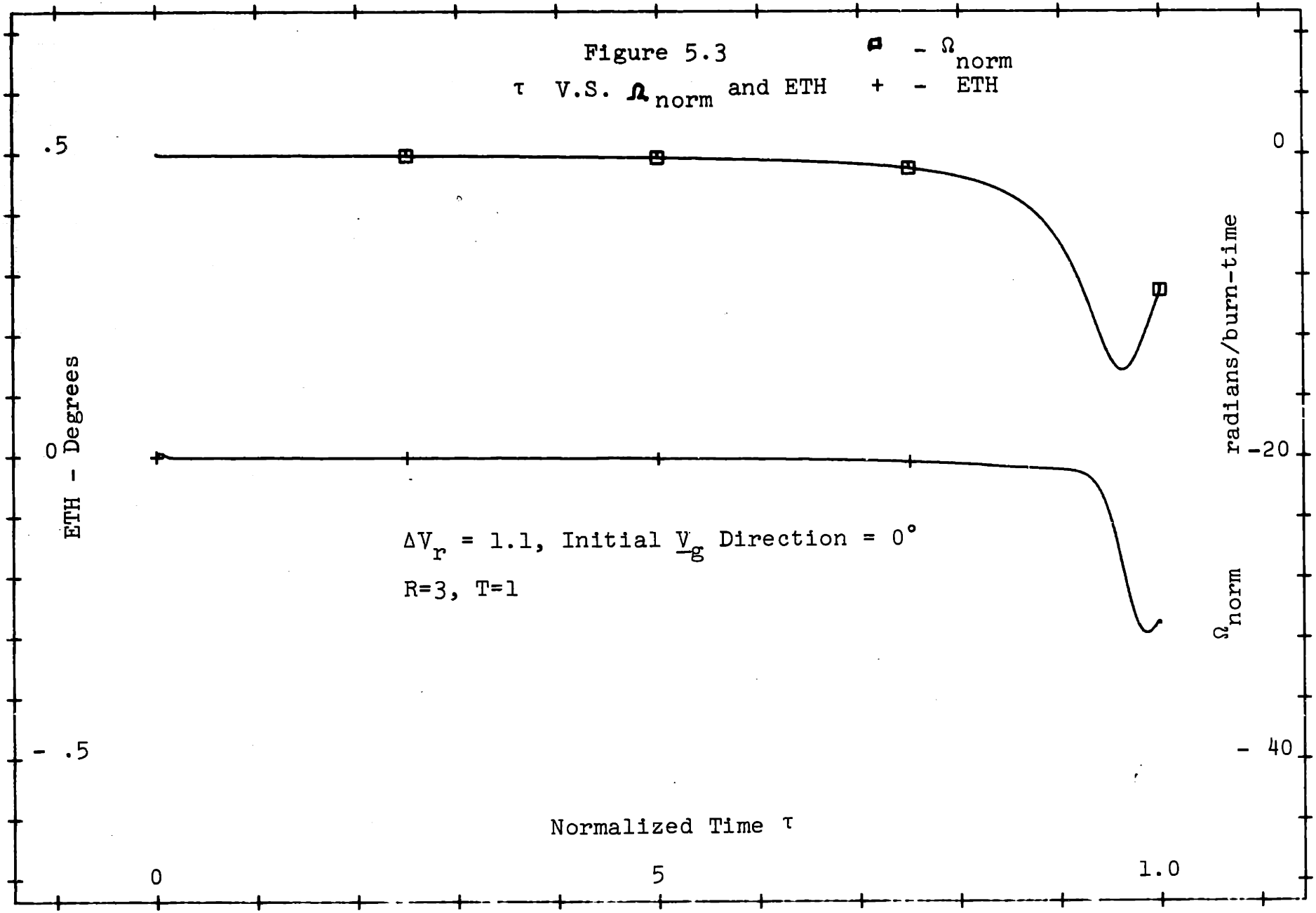
Figure 5.3
τ V.S. Ω norm and ETH
- Ω norm
+ - ETH
.5
0
- .5
ETH - Degrees
0
-20
- 40
radians/burn-time
Ω norm
ΔV r = 1.1, Initial V g Direction = 0°
R=3, T=1
Normalized Time τ
0
5
1.0

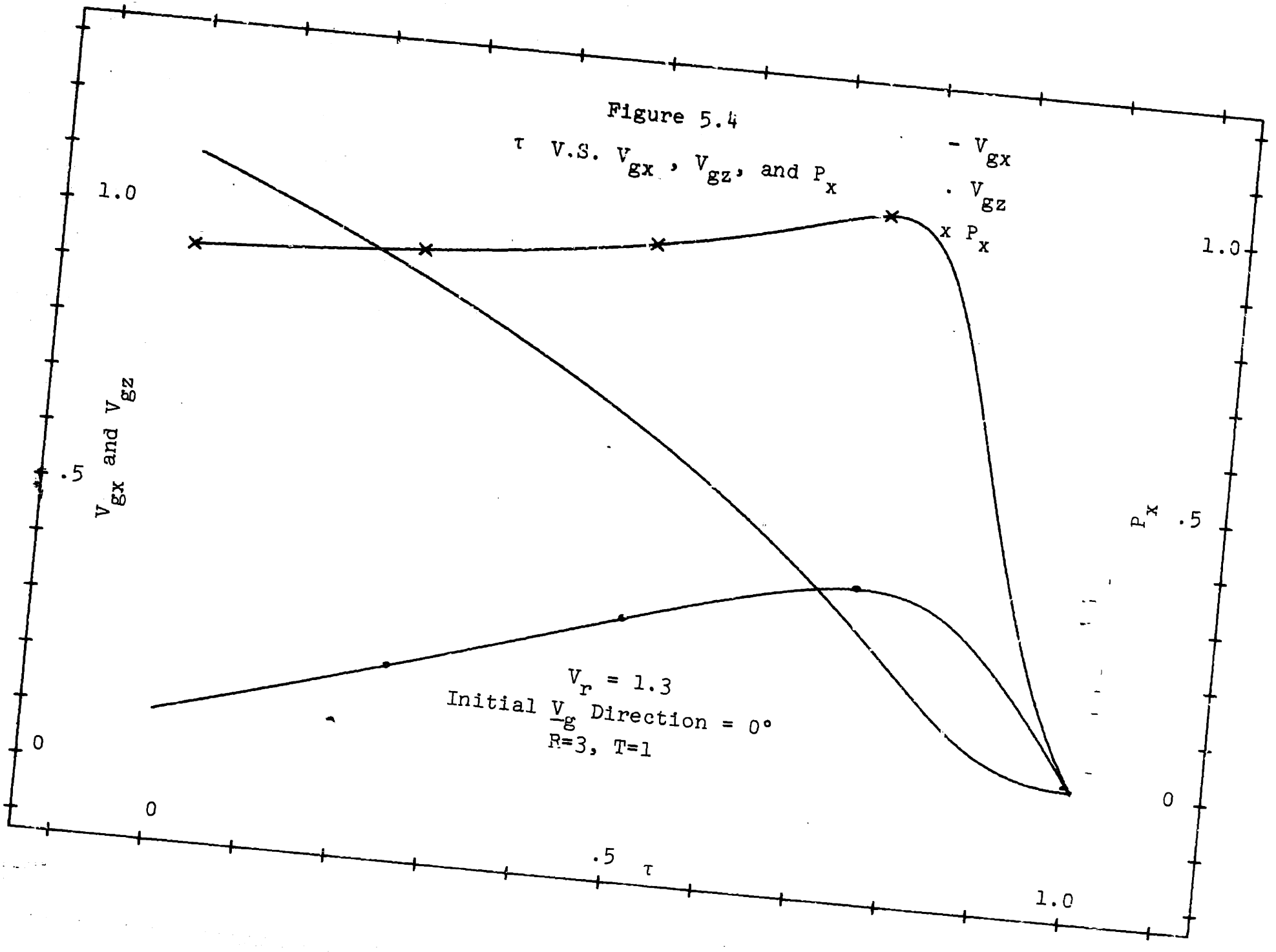
Figure 5.4
τ V.S. V_{gx} , V_{gz}, and P_x
- V_{gx}
. V_{gz}
x P_x
1.0
.5
0
V_{gx} and V_{gz}
P_x
V_r = 1.3
Initial $\underline{V}_g$ Direction = 0°
R=3, T=1
0
.5
τ
1.0

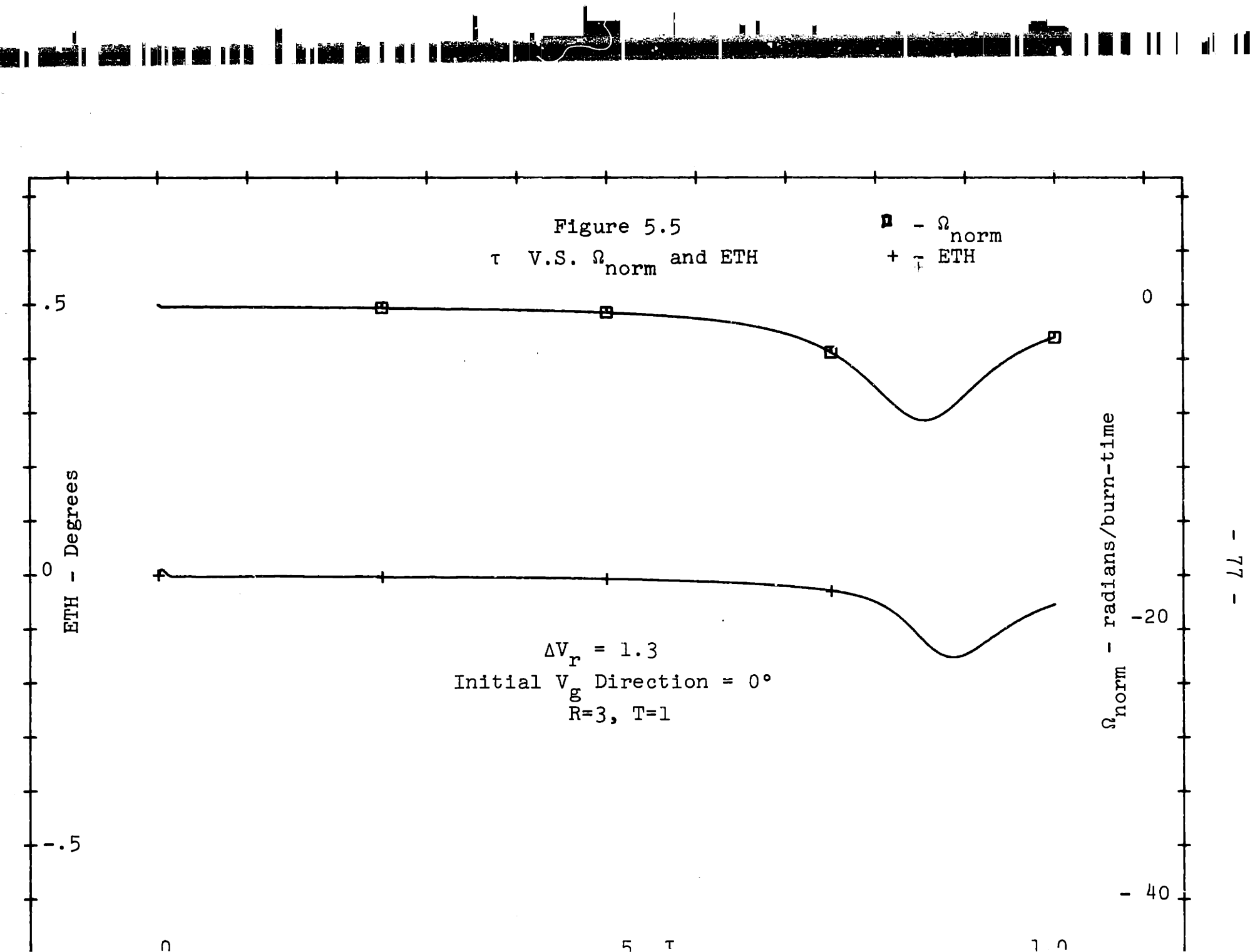
Figure 5.5
τ V.S. Ω_{norm} and ETH
- Ω_{norm}
+ ETH
.5
0
-.5
ETH - Degrees
0
-20
- 40
Ω_{norm} - radians/burn-time
ΔV_r = 1.3
Initial V_g Direction = 0°
R=3, T=1
0
.5
1.0
τ

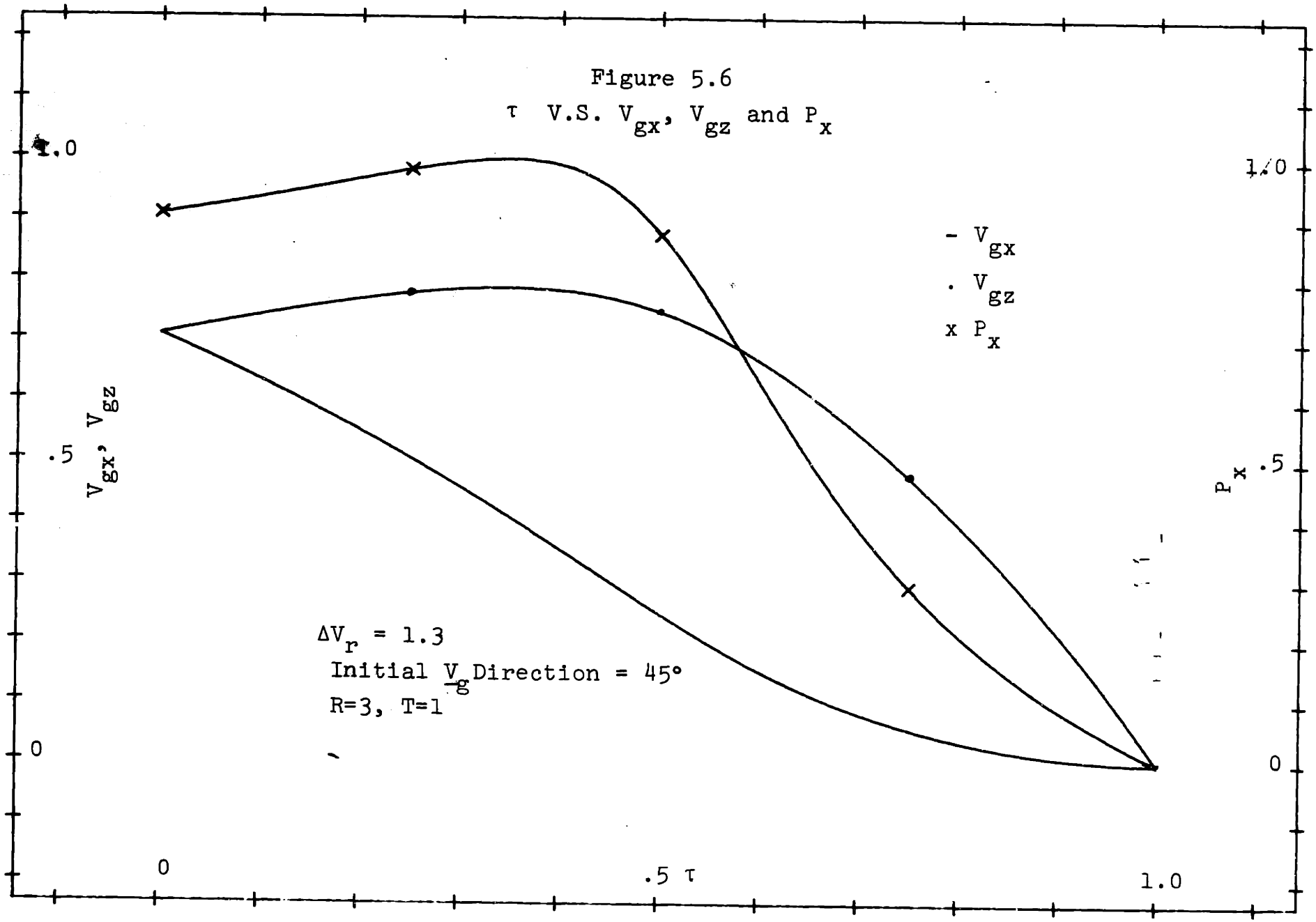
Figure 5.6
τ V.S. V_{gx}, V_{gz} and P_x
1.0
.5
0
V_{gx}, V_{gz}
- V_{gx}
. V_{gz}
x P_x
P_x
ΔV_r = 1.3
Initial $\underline{V}_g$ Direction = 45°
R=3, T=1
0
.5 τ
1.0

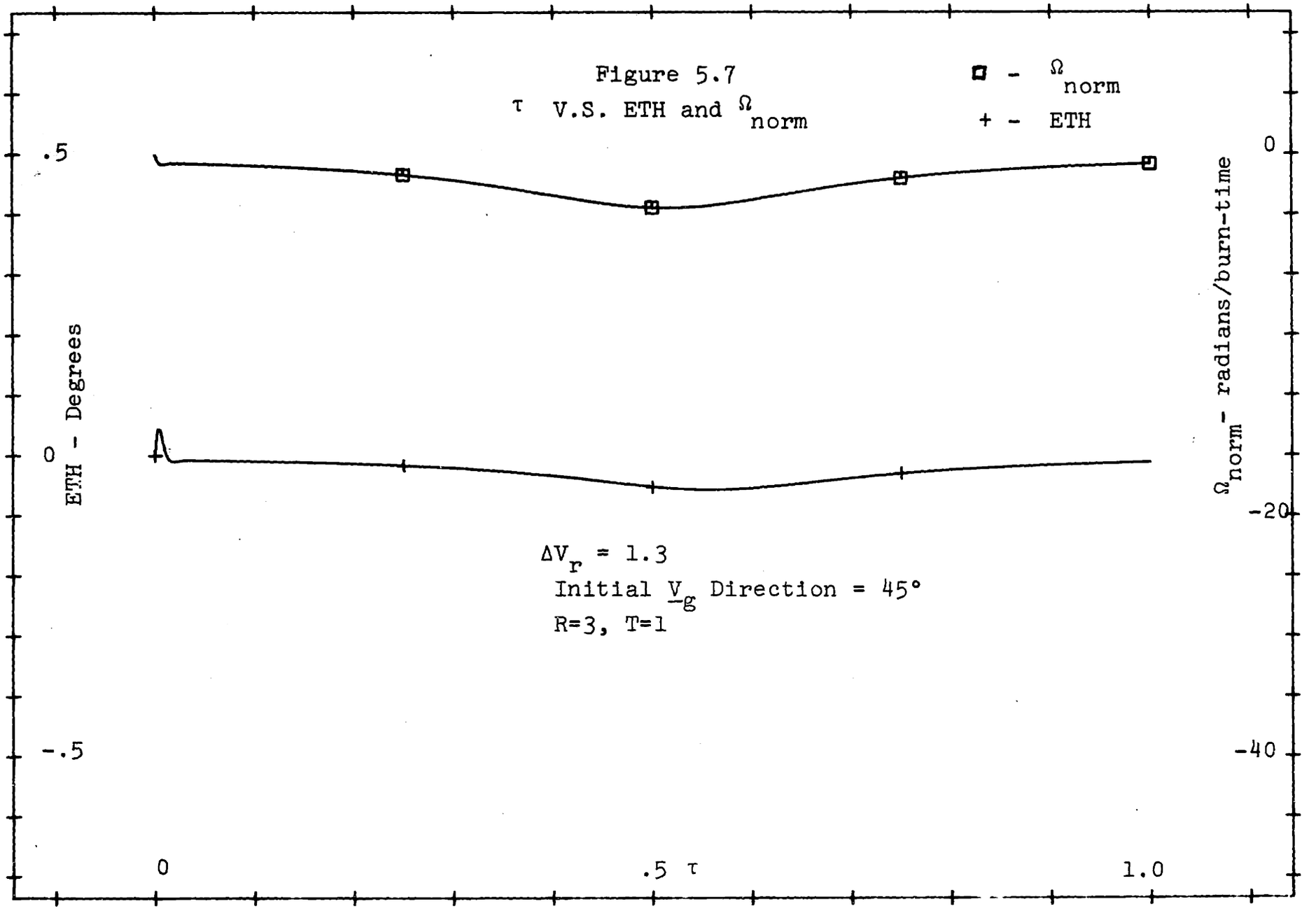
Figure 5.7
τ V.S. ETH and Ω norm
□ - Ω norm
+ - ETH
.5
0
-.5
ETH - Degrees
0
-20
-40
Ω norm - radians/burn-time
0
.5 τ
1.0
ΔV r = 1.3
Initial V g Direction = 45°
R=3, T=1

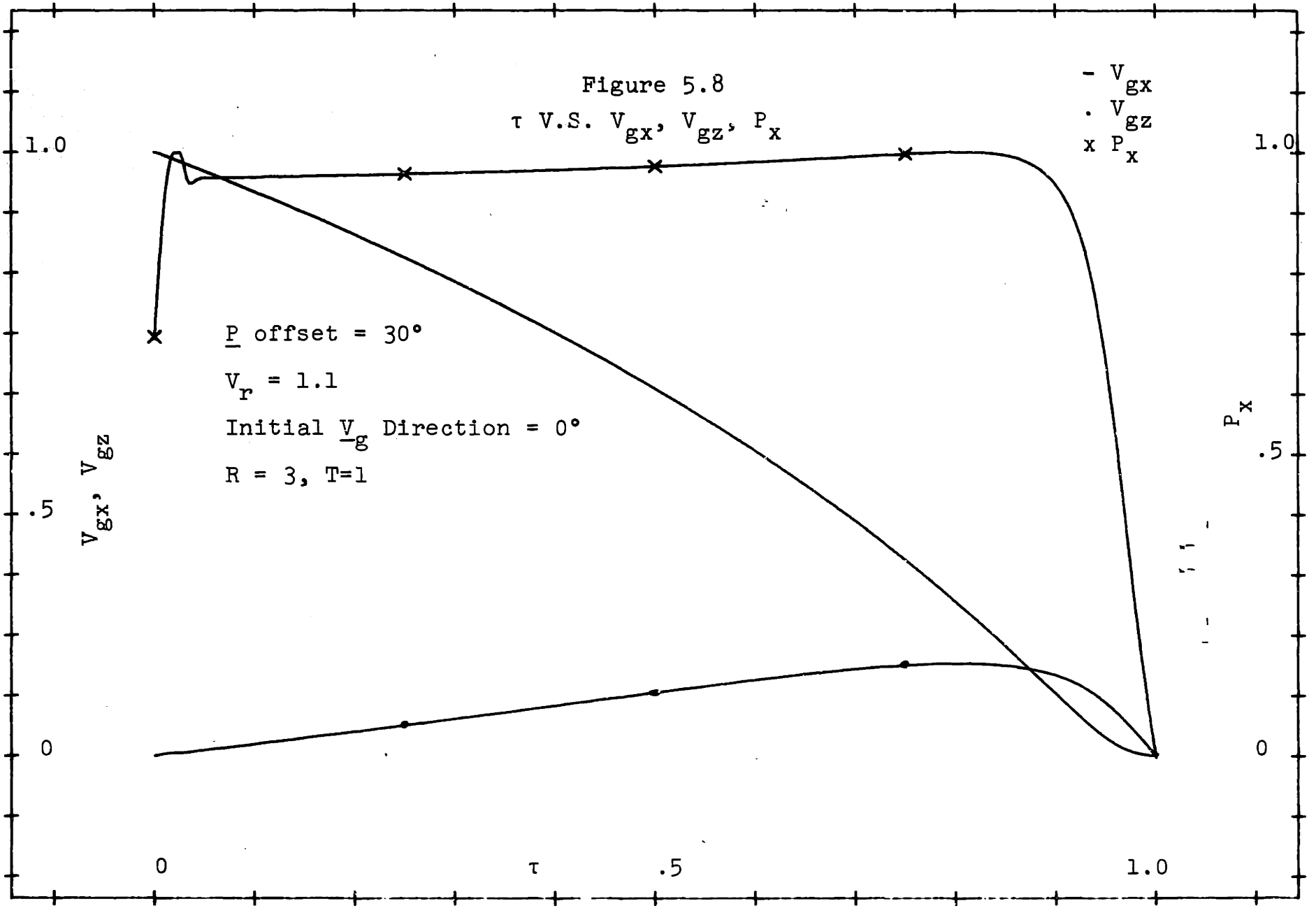
Figure 5.8
τ V.S. V_{gx}, V_{gz}, P_x
- V_{gx}
· V_{gz}
x P_x
P offset = 30°
V_r = 1.1
Initial V_g Direction = 0°
R = 3, T=1
1.0
.5
0
V_{gx}, V_{gz}
P_x
0
τ
.5
1.0

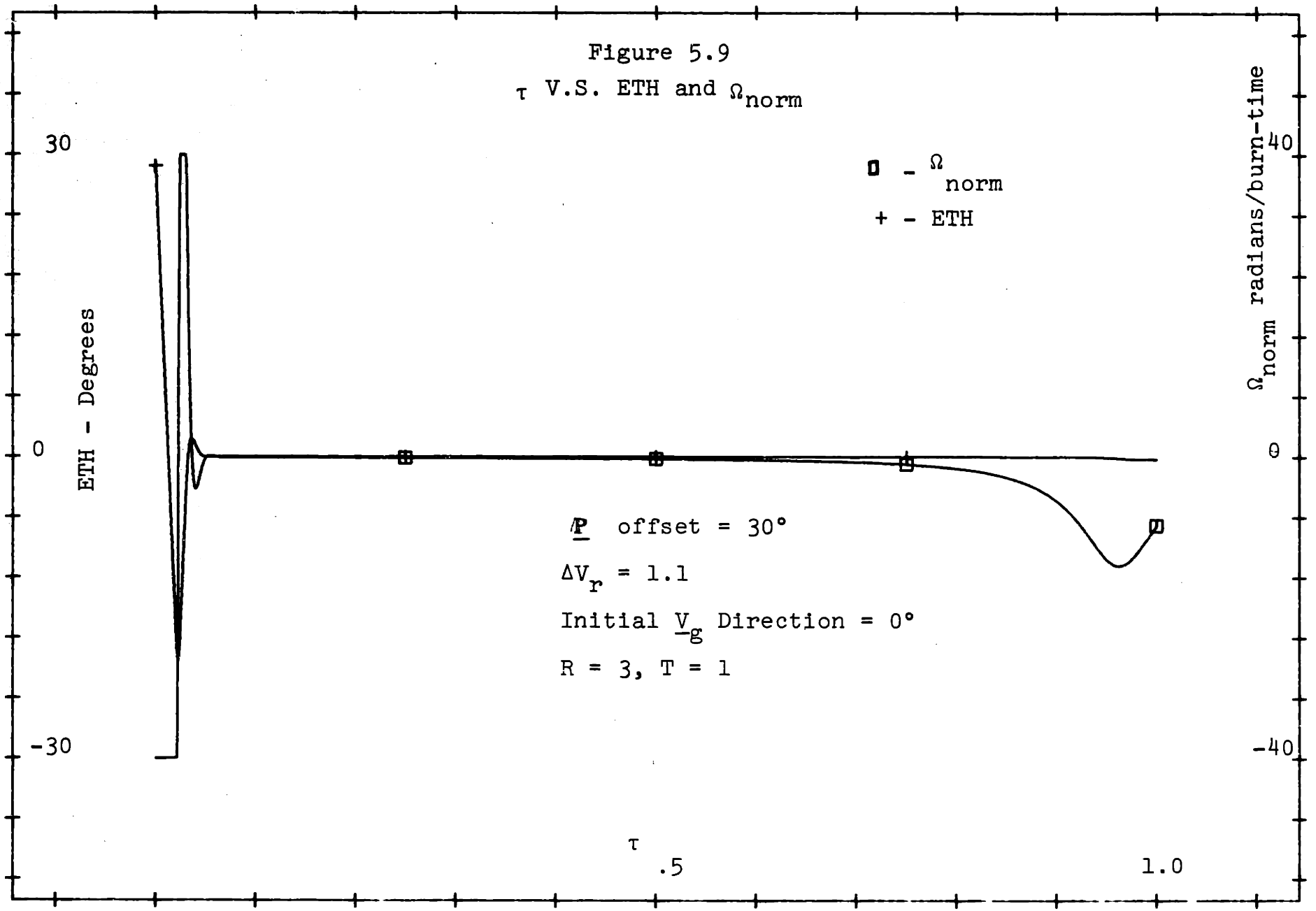
Figure 5.9
τ V.S. ETH and Ω norm
30
0
-30
ETH - Degrees
□ - Ω norm
+ - ETH
P offset = 30°
ΔV r = 1.1
Initial V g Direction = 0°
R = 3, T = 1
τ
.5
1.0
40
0
-40
Ω norm radians/burn-time

3. The data presented does not reflect the problem of terminal settling.

4. The $Q\underline{V}_g$ perturbation is handled without any problem.

5. A slow parabola update interval of .25 seconds was found to be satisfactory.

6. Initial offsets such as the 30° case may be tolerated with proper autopilot response.

7. Regressive burning lowers terminal angular rates.

5.4 Optimal Specified Time Problem Results

The optimal specified burn time problem discussed in Chapter II was solved using a method of steepest descent iteration.[5] An example of a solution is presented here. The specifications of the problem were

$$V_{gx}(0) = 3500 \text{ ft/sec}$$
$$V_{gz}(0) = 700 \text{ ft/sec}$$
$$|\underline{a}_T| = 200 \text{ ft/sec} = \text{constant}$$
$$t_f = \text{burn time} = 20 \text{ sec}$$

The terminal constraints which were used are

$$\beta(t_f) = \frac{\pi}{2} \text{ radians}$$
$$(V_{gx}(t_f)-.1) = 0$$
$$(V_{gz}(t_f)-.1) = 0$$

The initial control $\Omega_0(t)$ which was assumed is

$$\Omega_0(t) = 0 \quad 0 \leq t \leq 15 \text{ sec}$$

$$\Omega_0(t) = .3 \text{ rad/sec} \quad 15 \text{ sec} \leq t \leq 20 \text{ sec}$$

The algorithm initially satisfied the constraints by starting the constraint gain C_p at .1 and incrementing by -1. until a maximum of 1 was reached. After satisfying the terminal constraints, the cost J was reduced by a specified amount ΔJ_s. The value used initially was -.001 rad/sec. When the actual linear change in cost was less than the ΔJ_s, ΔJ_s was set equal to the actual change.

The results of the run are shown in Figures 5.10 and 5.11. The initial control history $\Omega_0(t)$ is shown in Figure 5.11 along with the (t) after 70 iterations of the algorithm. The rms value of $\Omega(t)$ was reduced from .142 radian/sec to .126 radian/sec, a reduction of about 15%. Figure 5.10 displays the time histories of V_{gx}, V_{gz}, and β converging on their terminal values.

The problem solution for the specified time worked well. Viewing the problem of terminal angular velocity, a penalty function on the terminal Ω might have proved useful.

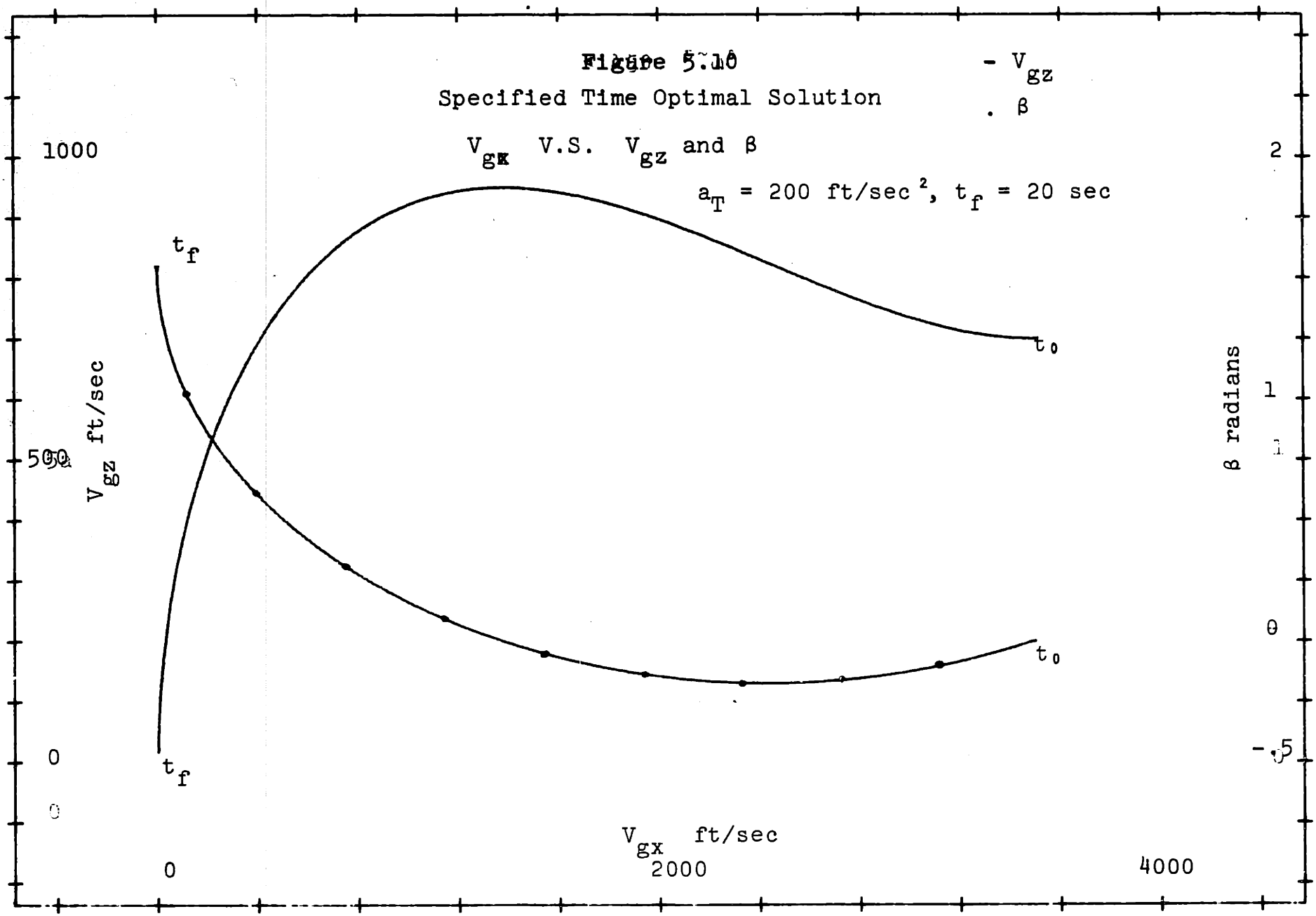
Figure 5.10
Specified Time Optimal Solution
V_{gx} V.S. V_{gz} and β
a_T = 200 ft/sec^2, t_f = 20 sec
- V_{gz}
. β
1000
500
0
V_{gz} ft/sec
t_f
t_f
t_0
t_0
0
2000
4000
V_{gx} ft/sec
2
1
0
-.5
β radians

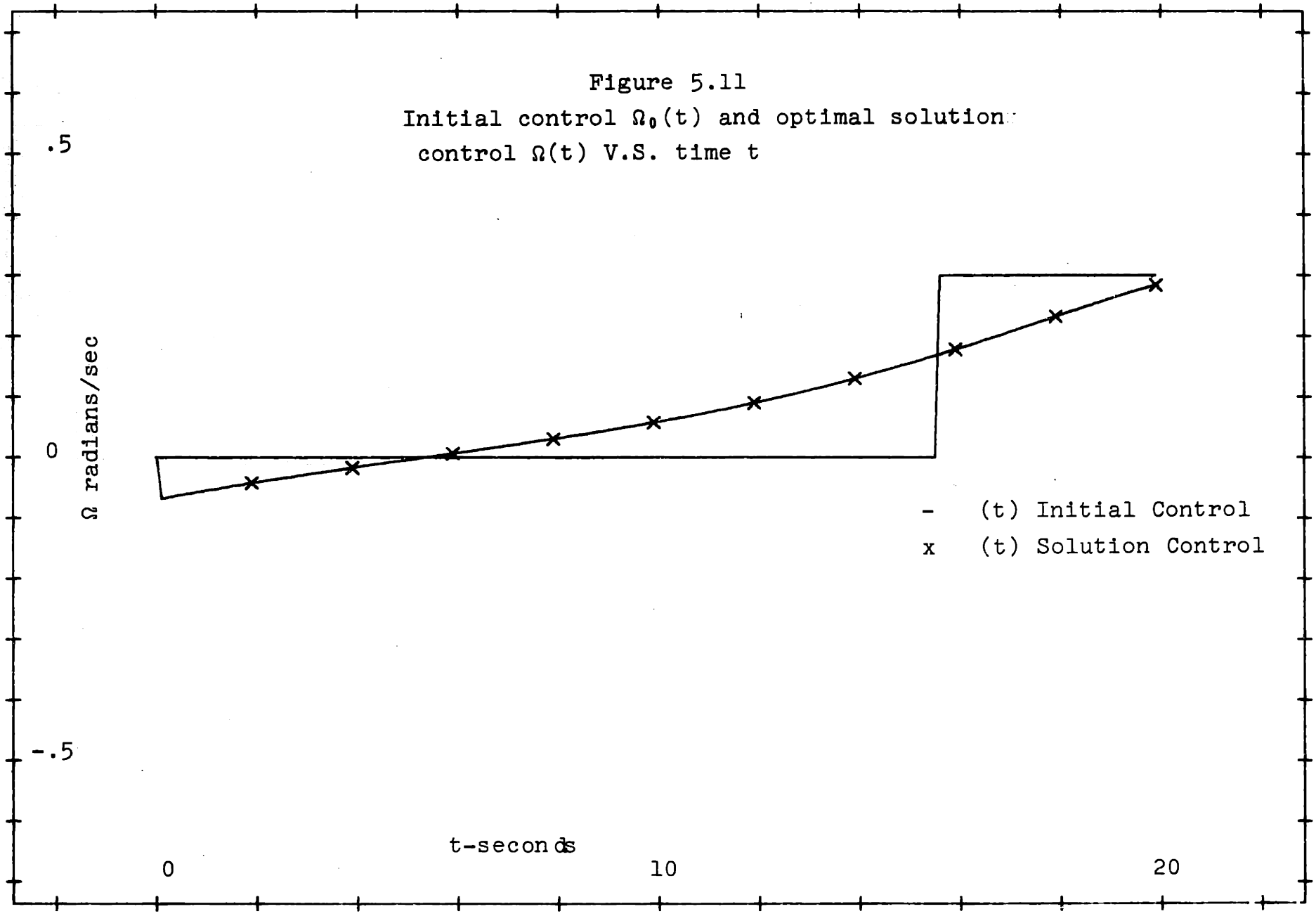

Figure 5.11
Initial control $\Omega_0(t)$ and optimal solution control $\Omega(t)$ V.S. time t

5.5 Conclusions

The parabolic guidance law proves to be acceptable in terms of computational complexity, flexibility, and autopilot requirements. The fact that it is explicit and closed loop in nature allows perturbations in initial conditions and thrust acceleration to be accommodated. Additional development of the steering law to follow the commanded trajectory is needed.

With additional development, the line-circle guidance technique should prove to be feasible. Guidance while on the circle arc is the major problem. The circle is less flexible than the parabola, and perturbations from the commanded trajectory result in either no solution being possible for the specified conditions, or the straight line segment direction varying rapidly.

5.6 Areas of Additional Work

1. The problem of settling into the I.S.D. direction while continuing to null $\underline{V}_g$ along this direction needs further development and analysis. Several approaches were discussed in Section 5.1.
2. The technique of thrusting along the $\underline{V}_g$ direction until a higher ΔV_r ratio is attained is a possible area of study.

3. The line-circle guidance technique with additional development of the guidance technique along the circular arc, should prove to be practical.

APPENDIX A

GRADIENT PROJECTION METHOD SOLUTION TO TWO POINT BOUNDARY VALUE PROBLEMS

1. Given initial conditions

$$\underline{x}(0) = \underline{x}_0 \tag{A.1}$$

$$J'(0) = 0 \tag{A.2}$$

2. Integrate from $0 \rightarrow T$

$$\underline{\dot{x}} = \underline{f}(\underline{x}) \tag{A.3}$$

$$\dot{J}' = \frac{1}{2}\Omega^2 \tag{A.4}$$

Using stored history of $\Omega(t)$

$$\Omega_{n+1}(t) = \Omega_n(t) - C_\psi\, G^T \Lambda\, I_{\psi\psi}^{-1} \underline{\psi}_n$$

$$-C_J \left[H_\psi - G^T \Lambda\, I_{\psi\psi}^{-1}\, I_{\psi J} \right] \tag{A.5}$$

Using from memory

$$H_\Omega{}^T,\ G^T \Lambda,\ \Omega_n(t)$$

3. Store

$$\Omega(t) \tag{A.6}$$

$$\underline{x}(t)$$

4. At T evaluate

$$J(T) = J^{*}(T) \tag{A.7a}$$

$$\psi\mu(T) = (x_1(T) - a,\ x_2(T) - b,\ x_3(T) - c) \tag{A.7b}$$

5. Exercise step size control if necessary

6. Test to stop

$$\underline{\psi}(T) = 0 \tag{A.8}$$

7. If $\underline{\psi} \neq 0$ Continue:

$$\underline{\lambda}(T) = 0 \tag{A.9}$$

$$\Lambda(T) = \frac{\partial \underline{\psi}^{T}}{\partial \underline{x}} \tag{A.10}$$

$$I_{JJ}(T) = 0 \tag{A.11}$$

$$I_{\psi J}(T) = 0 \tag{A.12}$$

$$I\psi\psi(T) = 0 \tag{A.13}$$

8. Integrate from T to 0 picking up from memory $\Omega(t), \underline{x}(t)^{t}$

$$\dot{\underline{\lambda}} = -F^{T} = 0 \tag{A.14}$$

$$\dot{\Lambda} = - F^T \Lambda \tag{A.15}$$

$$\dot{I}_{JJ} = -H_\Omega \tag{A.16}$$

$$H_\Omega = L_\Omega = \Omega \tag{A.17}$$

$$\dot{I}_{\psi J} = - \Lambda^T G H_\Omega{}^T \tag{A.18}$$

$$\dot{I}_{\psi\psi} = - \Lambda^T G G^T \Lambda \tag{A.19}$$

$$F = \frac{\partial \underline{f}}{\partial \underline{x}} \quad , \quad G = \frac{\partial \underline{f}}{\partial \Omega} \tag{A.20}$$

9. Store $H_\Omega(t)$; $G^T \Lambda(t)$

10. At $t = 0$, evaluate

$$I_{\psi\psi}{}^{-1} \underline{\psi} \ , \ I_{\psi\psi}{}^{-1} \quad I_{\psi J} \tag{A.21}$$

11. Step Size Control

Choose C_ψ, C_J where C_ψ is the control for the constraints and C_J is control for cost change in J.

(a) Start C_J small and increment to 1

(b) $$C_J = \frac{-\Delta J_s - C_\psi \ I_{\psi J}{}^T \ I_{\psi\psi}{}^{-1} \psi}{I_{JJ} - I_{\psi J}{}^T I_{\psi\psi}{}^{-1} I_{\psi J}} \tag{A.22}$$

where ΔJ_s is the specified change in the cost.

If $C_J < 0$, set $C_J = 0$

Toward solution point, denominator of A.22 $\rightarrow$ 0. Then let C_J = constant.

(c) With large increase in cost - cut back on C_J

12. Repeat cycle

REFERENCES

1. Laning, J. H. and Battin, R. H., "Theoretical Principle for a Class of Inertial Guidance Computers for Ballistic Missiles," M.I.T. Instrumentation Laboratory Report R-125, June 1956 (Conf.).

2. Turano, R. L., "Steering Control for a Final Stage Low Thrust Vehicle," (Conf.), M.I.T. Masters Thesis, 1965.

3. Bryson, A. E. and Ho, Yu-Chi, "Applied Optimal Control," Ginn-Blaisdell, Waltham, Massachusetts, 1969.

4. Wheelon, A.D., "Free Flight of a Ballistic Missile," A R S Journal, December 1959.

5. Class notes from course 16.39 on optimal control taught at M.I.T. in the Fall semester, 1970.

BIBLIOGRAPHY

1. Athans, M. and Falb, P. L., "Optimal Control," McGraw-Hill, New York, 1966.

2. Martin, F. H., "Closed-Loop Near-Optimum Steering for a Class of Space Missions"